

A Fenchel-Young Loss Approach to Data-Driven Inverse Optimization

Zhehao Li*

Tsinghua University, 100084 Beijing, China, lizh21@mails.tsinghua.edu.cn

Yanchen Wu*

Tsinghua University, 100084 Beijing, China, wu-yc23@mails.tsinghua.edu.cn

Xiaojie Mao[†]

Tsinghua University, 100084 Beijing, China, maobj@sem.tsinghua.edu.cn

Data-driven inverse optimization seeks to estimate unknown parameters in an optimization model from observations of optimization solutions. Many existing methods are ineffective in handling noisy and suboptimal solution observations and also suffer from computational challenges. In this paper, we build a connection between inverse optimization and the Fenchel-Young (FY) loss originally designed for structured prediction, proposing a FY loss approach to data-driven inverse optimization. This new approach is amenable to efficient gradient-based optimization, hence much more efficient than existing methods. We provide theoretical guarantees for the proposed method and use extensive simulation and real-data experiments to demonstrate its significant advantage in parameter estimation accuracy, decision error and computational speed.

1. Introduction

Inverse optimization is a fundamental problem in operations research and machine learning, aiming to estimate unknown parameters in an optimization model from observations of solutions (Ahuja and Orlin 2001). Inverse optimization is important in many applications, such as consumer utility modeling (Saez-Gallego et al. 2016, Saez-Gallego and Morales 2017), vehicle routing (Chen et al. 2021, Zattoni Scroccaro et al. 2024), medical decision-making (Chan et al. 2014, Aswani et al. 2019), and portfolio risk management (Li 2021, Yu et al. 2023), etc. For example, in the consumer utility modeling problem, customers' utility function may involve unknown parameters characterizing their preference for different products. These parameters may be estimated from observations of utility-maximizing customers' purchase decisions. By recovering the unknown parameters in the optimization, analysts can better understand the underlying decision-making process and make better decisions of their interest.

In data-driven inverse optimization, the observed decisions may be often noisy, suboptimal and even infeasible, which poses significant challenges for estimating the unknown parameters (Chan et al.

* These authors contributed equally to this work.

[†] Corresponding author.

2023). Aswani et al. (2018) discovered that many existing approaches may not effectively recover the true parameter value, such as the Karush-Kuhn-Tucker approximation (KKA) approach (Keshavarz et al. 2011) and the variational inequality approximation (VIA) approach (Bertsimas et al. 2015). Aswani et al. (2018) then proposed a parameter estimator such that the average squared distance between the decision induced by the estimated parameter and the observed decision is minimized and showed its effectiveness theoretically and numerically. However, this approach involves non-convex optimization solved by brute-force enumeration, restricted to only small-scale problems. For larger problems, Aswani et al. (2018) relied on a semiparametric approach that is more scalable than enumeration. However, this approach it is not amenable to first-order gradient-based optimization, hence still computationally challenging for large-scale problems.

In this paper, we propose an alternative surrogate loss function approach to overcome the drawbacks of existing methods. Specifically, we consider a regularized version of the optimization problem of interest and adapt the suboptimality loss in Chan et al. (2014), Chan and Lee (2018) to the regularized problem. We find that the resulting loss coincides with the Fenchel-Young (FY) loss originally designed for structured prediction tasks such as classification and ranking (Blondel et al. 2020, 2022). This builds a novel connection between FY loss and data-driven inverse optimization, providing new perspectives on both. Importantly, the FY loss is differentiable with a closed-form gradient and it is convex for linear problems. This allows for efficient first-order optimization like stochastic gradient descent (SGD), thereby achieving significant computational advantage over existing methods. By extending existing FY loss theory, we also provide some theoretical guarantees for the proposed method. We evaluate our method on synthetic and real-world datasets, demonstrating that our approach outperforms existing methods in terms of parameter estimation accuracy, generating high quality decisions, and computational efficiency. In particular, the proposed method can achieve robust performance even in settings where existing methods easily give degenerate solutions.

1.1. Related Work

Inverse Optimization Early work on inverse optimization focused on parameter recovery from noiseless observations of decision solutions (Ahuja and Orlin 2001, Chan et al. 2014, Chan and Lee 2018). Bärmann et al. (2017) studied inverse optimization with noiseless solutions in the online setting, focusing on minimizing decision suboptimality, while Besbes et al. (2023) aimed to estimate parameters by minimizing worst-case regret. To handle noisy and suboptimal decisions in data-driven inverse-optimization, Aswani et al. (2018) proposed a squared distance loss approach and a semiparametric approach and compared their methods with methods in Keshavarz et al. (2011), Bertsimas et al. (2015). Their methods were also expanded to the online setting (Dong et al. 2018). Chan et al. (2019) proposed a goodness-of-fit measure for data-driven inverse-optimization. We refer

to Chan et al. (2023) for a comprehensive survey of literature on classical inverse optimization and data-driven inverse optimization and, Mohajerin Esfahani et al. (2018), Birge et al. (2022), Lin et al. (2024) for some recent advances in enhancing the robustness of inverse optimization methods. Our paper considers the offline setting in Aswani et al. (2018) and proposes a Fenchel-Young loss approach to inverse optimization, addressing the computational challenges with existing methods while achieving rigorous theoretical guarantees.

Structured Prediction with FY Loss The Fenchel-Young (FY) loss was originally introduced for structured prediction (SP) tasks such as multi-class classification and ranking (e.g., Blondel et al. 2019, 2020, 2022). We refer to Blondel et al. (2020) for a systematic introduction to FY loss. In this paper, we build the connection between FY loss and data-driven inverse-optimization. Our methodology and theory build on and extend the FY loss literature, broadening the applicability of FY loss. In particular, the traditional structured prediction tasks for which FY loss is designed typically involve optimization or ranking over simple sets like simplex, while inverse optimization may often involve operations problems with more complex structure.

2. Problem Formulation

2.1. Forward and Inverse Optimization

In this paper, we study the inverse linear optimization problem with noisy observed decisions. Let $x \in \mathbb{R}^d$ be the decision vector, $u \in \mathbb{R}^m$ the context variable, and $\theta^* \in \mathbb{R}^p$ the unknown parameter vector to be estimated. The forward optimization problem (FOP) is given by:

$$\text{FOP}(\theta^*, u) := \max_x \{h(\theta^*; u)^\top x \mid g(u, x) \preceq 0\}. \quad (1)$$

Here $h : \mathbb{R}^p \times \mathbb{R}^m \rightarrow \mathbb{R}^d$ represents the cost function, and function $g : \mathbb{R}^m \times \mathbb{R}^d \rightarrow \mathbb{R}^q$ defines the constraints. Both h and g are assumed known, leaving θ^* as the only unknown parameter. We define the feasible region of FOP as $\mathcal{X}(u) := \{x \in \mathbb{R}^d \mid g(u, x) \preceq 0\}$, and use $x^*(\theta^*; u) \in \mathcal{X}^*(\theta^*; u)$ to denote a generic optimal solution of $\text{FOP}(\theta^*, u)$, where $\mathcal{X}^*(\theta; u) := \arg \max_x \{h(\theta; u)^\top x \mid g(u, x) \preceq 0\}$ is the optimal solution set.

We assume that $h(\theta; u)$ is continuous in θ and u , while $g(u, x)$ is continuous in both u and x and convex in x for each fixed u . These conditions mean that the FOP in Equation (1) has a linear objective with convex constraints¹. Such formulation is widely studied in the inverse optimization literature (Bertsimas et al. 2015, Bärman et al. 2017, Aswani et al. 2018, Chen et al. 2021, Yu

¹While we focus on linear objectives in the main text, our method can be also applied to nonlinear objectives; see the numerical experiments in Section EC.4.

et al. 2023). Additional examples that align with our formulation in Equation (1) are provided in Section EC.1.

Noisy Observations Suppose $(U, Y) \in \mathbb{R}^m \times \mathbb{R}^d$ is a pair of context-decision variables, sampled from an unknown joint distribution P . Here Y stands for the noisy observation of the true decision $x^*(\theta^*; U)$ under the context U with the unknown parameter θ^* . We assume observing a sequence of noisy data $\{(U_i, Y_i)\}_{i=1}^n$ drawn identically and independently (IID) from the joint distribution P .

ASSUMPTION 1 (Noisy Decisions). *For each $i \in [n]$, we assume $Y_i = x^*(\theta^*; U_i) + W_i$. The noise terms $\{W_i\}_{i=1}^n$ are IID with zero conditional mean and finite conditional variance given context $u \in \mathbb{R}^m$, i.e., $\mathbb{E}[W_i | U = u] = 0$ and $\text{Var}[W_i | U = u] < \infty$. Meanwhile, W_i is independent of U_i for each $i \in [n]$.*

As highlighted in Aswani et al. (2018), accounting for noise in inverse optimization is crucial, as real-world decisions are often influenced by various sources of noise. This noise can arise from (i) measurement errors in the data collection process, (ii) deviations of experts from optimal behavior, or (iii) discrepancies between the parametric FOP model and the true underlying decision-making process.

REMARK 1 (NOISE MODEL). In this paper, we follow Aswani et al. (2018) and focus on the noisy decisions setting in Assumption 1. An alternative noisy model is to incorporate noise in the optimization objective, i.e., we observe $Y_i \in \arg \max_{x \in \mathcal{X}(U_i)} \{(h(\theta^*; U_i) + W_i)^\top x\}$ for each $i \in [n]$. Our experiments in Section EC.4 also examine this noisy objective setting and demonstrate that our proposed method also outperforms existing methods in this setting.

Data-driven Inverse Optimization Given a sequence of data $\{(U_i, Y_i)\}_{i=1}^n$, the goal of inverse optimization is to estimate the unknown parameter θ^* from data. The ultimate aim is to leverage the estimated parameter, denoted as $\hat{\theta}$, to make new decisions in subsequent contexts. Therefore, it is desirable to ensure that the optimal decision $x^*(\hat{\theta}; U)$ is, on average, as close as possible to the observed decision Y . To achieve this goal, Aswani et al. (2018) then proposed to minimize the risk associated with the inverse optimization problem (IOP):

$$\min_{\theta \in \Theta} R_{\text{DIST}}(\theta) := \mathbb{E}[L_{\text{DIST}}(\theta; U, Y)], \quad (2)$$

where $\Theta \in \mathbb{R}^p$ and L_{DIST} is the squared distance loss:

$$L_{\text{DIST}}(\theta; U, Y) := \min_{x \in \mathcal{X}^*(\theta; U)} \|Y - x\|_2^2, \quad (3)$$

which quantifies the deviation of the optimal solution set $\mathcal{X}^*(\theta; U)$ from the observed decision Y under the context U . Assumption 1 guarantees that the true unknown parameter θ^* minimizes the

risk $R_{\text{DIST}}(\theta)$ (Aswani et al. 2018). As an alternative to the IOP formulation in Equation (2), we can consider minimizing the excess risk $R_{\text{DIST}}(\theta) - R_{\text{DIST}}(\theta^*)$ over θ . It turns out that the excess risk is equivalent to the expected decision error (defined below) over the distribution of U when the optimal solution of FOP with respect to any given parameter θ is almost surely unique.

ASSUMPTION 2 (Almost Sure Uniqueness, Aswani et al. (2018), IC condition). *For any $\theta \in \Theta$ and $u \in \mathbb{R}^m$, $\text{FOP}(\theta, u)$ has a unique optimal solution almost surely, that is, $\mathcal{X}^*(\theta; u) = \{x^*(\theta; u)\}$ almost surely.*

Assumption 2 is a common assumption (Aswani et al. 2018, Elmachtoub and Grigas 2022) and holds automatically when the context U follows a continuous distribution and the constraint set $\mathcal{X}(u)$ is a polytope.

LEMMA 1. *Given Assumptions 1 and 2, we have*

$$R_{\text{DIST}}(\theta) - R_{\text{DIST}}(\theta^*) = \mathbb{E}[\|x^*(\theta; U) - x^*(\theta^*; U)\|_2^2], \quad \forall \theta \in \Theta.$$

Lemma 1 shows that, when choosing the squared distance loss in Equation (3), minimizing the IOP risk $R(\theta)$ over Θ is equivalent to minimizing the expected *decision error*

$$D(\theta, \theta^*) := \mathbb{E}[\|x^*(\theta; U) - x^*(\theta^*; U)\|_2^2], \quad (4)$$

which is the expectation of the squared distance between the optimal solutions $x^*(\theta; U)$ and $x^*(\theta^*; U)$ over the distribution of U . If a parameter θ can achieve a small expected decision error, then the decision induced by θ would achieve a small *decision regret* relative to the decision induced by the true parameter θ^* :

$$\text{Reg}(\theta, \theta^*) := \mathbb{E}[h(\theta^*; U)^\top (x^*(\theta; U) - x^*(\theta^*; U))]. \quad (5)$$

In Theorem 4, we show that the decision regret above can be upper bounded by the expected decision error. If we further assume a separation condition as formalized in Aswani et al. (2018, IC condition), then we can also bound the following *parameter error* through the decision error $D(\theta, \theta^*)$:

$$E(\theta, \theta^*) := \|\theta - \theta^*\|_1. \quad (6)$$

The parameter error is defined as the distance between a given parameter θ and the true unknown parameter θ^* with respect to the l_q -norm on the \mathbb{R}^p space. Without loss of generality, we choose $q = 1$ for the parameter error $E(\theta, \theta^*)$ as shown in Eq. (6).

Empirical Risk Minimization (ERM) with Distance Loss Aswani et al. (2018) propose to minimize the empirical risk with the squared distance loss in Equation (3) over a parameter space Θ :

$$\min_{\theta \in \Theta} \widehat{R}_{\text{DIST}}(\theta) := \frac{1}{n} \sum_{i=1}^n L_{\text{DIST}}(\theta; U_i, Y_i). \quad (7)$$

However, directly minimizing the empirical risk in Equation (7) presents challenges, as the distance loss L_{DIST} is neither convex nor differentiable with respect to the parameter θ , even under Assumption 2. Aswani et al. (2018) therefore proposed an enumeration algorithm that computes the value of $\widehat{R}_{\text{DIST}}(\theta)$ for each θ over a discretized grid of Θ , which is computationally expensive when facing the high-dimensional parameter. Meanwhile, the complexity of computing $\widehat{R}_{\text{DIST}}(\theta)$ scales significantly with the sample size and decision dimension, further exacerbating computational challenges.

The next subsection will describe several existing alternatives to the distance loss L_{DIST} . To more clearly illustrate properties of these losses, we now assume the cost function $h(\theta; u)$ is linear in the parameter θ . This is the most common setting considered in the existing inverse optimization literature (e.g., Chan et al. 2014, Bärman et al. 2017, Chen et al. 2021, Besbes et al. 2023, Sun et al. 2023). All numeric examples in Aswani et al. (2018) and Examples EC.1 and EC.2 also satisfy this linearity condition.

ASSUMPTION 3 (Linear Cost). *The cost function $h(\theta; u)$ is linear in the unknown parameter θ for each context $u \in \mathbb{R}^m$, i.e., $h(\theta; u) = A(u)\theta$ for some feature mapping $A(u)$.*

2.2. Loss Functions for Inverse Optimization

The distance loss L_{DIST} is not the only choice for the inverse optimization in Equation (2) via empirical risk minimization. We briefly summarize other loss functions in the existing literature, and leave the comprehensive discussion to Section EC.1.3.

KKT-Approximated Loss Keshavarz et al. (2011) proposed a loss for a noiseless decision setting that measures the violation of the Karush-Kuhn-Tucker (KKT) conditions:

$$L_{\text{KKA}}(\theta; u, y) := \min_{\lambda \geq 0} \{L_{\text{ST}}(\theta; u, y, \lambda) + L_{\text{CS}}(u, y, \lambda)\},$$

where L_{ST} and L_{CS} capture the magnitude of the violation of *stationary condition* and *complementary slackness*, respectively. In noisy setting, minimizing the empirical IOP risk with L_{KKA} is challenging, as observed decisions may be infeasible, leading to large violations of KKT conditions.

Suboptimality Loss Chan et al. (2014), Chan and Lee (2018), Chan et al. (2019) proposed to estimate the parameters by minimizing the average duality gap between the dual optimal objective $v(\theta; \lambda_i, U_i)$ induced by the parameter and the objective function of observed decisions:

$$\min_{\theta, \epsilon_i, \lambda_i \geq 0, i=1, \dots, n} \frac{1}{n} \sum_{i=1}^n \epsilon_i \text{ s.t. } v(\theta; \lambda_i, U_i) - h(\theta; U_i)^\top Y_i \leq \epsilon_i. \quad (8)$$

Chan et al. (2023) points out that Equation (8) is equivalent to minimizing the empirical risk $\widehat{R}(\theta)$ in Equation (7) with the loss replaced by the *suboptimality loss* as follows:

$$L_{\text{SUB}}(\theta; u, y) := \max_{x \in \mathcal{X}(u)} h(\theta; u)^\top x - h(\theta; u)^\top y. \quad (9)$$

Although the optimization problem in this approach is convex and tractable, this duality-based approach still faces several challenges. (1) If there exists a parameter $\theta \in \Theta$ such that $h(\theta; u) = 0$, then the suboptimality loss L_{SUB} also reaches zero at this θ , causing the inverse optimization problem to degenerate. (2) As the sample size and decision dimension increase, the dual formulation of Equation (8) becomes computationally challenging. (3) It is unknown whether ERM with the suboptimality loss can control the decision error in Equation (4).

Variational Inequality Loss Bertsimas et al. (2015) study the variational inequality approximation (VIA) loss function that measures the optimality margin for the FOP with a differentiable objective function $f(\theta; u, x)$:

$$L_{\text{VIA}}(\theta; u, y) = \max_{x \in \mathcal{X}(u)} \nabla_y f(\theta; u, y)^\top (x - y). \quad (10)$$

If the objective function is linear in decision x , e.g., $f(\theta; u, x) = h(\theta; u)^\top x$, the VIA loss simplifies to the suboptimality loss, inheriting the same challenges.

Semi-parametric Methods To overcome the limitations of squared distance loss with large problems, Aswani et al. (2018) propose a semi-parametric (SPA) method that first uses the Nadaraya-Watson (NW) estimator to denoise the observed decisions and then projects them onto the feasible region, denoted as \tilde{Y}_i . Aswani et al. (2018) then propose to solve Equation (8) by replacing Y_i with \tilde{X}_i for each $i \in [n]$. However, the NW estimator performs poorly with high-dimensional context space, and they also employ a dual formulation that is computationally challenging to optimize when the sample size and dimension are large.

Challenges for Existing Loss Functions Existing loss functions face several key challenges: difficulty with handling noisy observations, degeneracy, and computational bottleneck. Moreover, most of these methods, except the distance loss and semi-parametric method proposed in (Aswani et al. 2018), do not provide direct control over the expected decision error $D(\theta, \theta^*)$ in Equation (4) and parameter error $E(\theta, \theta^*)$ in Equation (6). In this paper, we propose a surrogate loss that is computationally efficient, robust to both noise and degeneracy, and retains statistical guarantees for error control.

3. Inverse Optimization with FY Loss

In this section, we first define the regularized forward optimization problem (R-FOP) by introducing a strongly-convex regularizer, and then connect the suboptimality loss for the R-FOP with the Fenchel-Young (FY) loss. The excess risk induced by FY loss also provides a direct control of the decision error $D(\theta, \theta^*)$ for any parameter θ . The convexity and differentiability of FY loss enable us to apply a gradient-based algorithm that is particularly suitable for large sample size and high-dimensional problem.

3.1. Regularized Optimization and Fenchel-Young Loss

Since we consider a linear FOP in Equation (1), the optimal solution $x^*(\theta; u) \in \mathcal{X}^*(\theta; u)$ may not be unique for a given θ and u unless Assumption 2 holds. Moreover, $x^*(\theta; u)$ is generally non-smooth with respect to θ for a fixed context $u \in \mathbb{R}^m$, implying that the sub-gradients $\partial_\theta x^*(\theta; u)$ may not exist. Additionally, the decision error $D(\theta, \theta^*)$ in Equation (4) is non-convex in θ even if $x^*(\theta; u)$ is convex in θ for every fixed context u , since $D(\theta, \theta^*)$ is not monotonic in x^* and convexity in θ is not preserved under composition Boyd (2004). These challenges prevent the direct application of gradient-based methods to minimize $D(\theta, \theta^*)$ for θ over the parameter space $\Theta \subseteq \mathbb{R}^p$.

In view of these issues, we introduce a regularized version of the FOP in Equation (1) by adding a 1-strongly-convex regularizer Ω , for example, $\Omega(x) = \|x\|_2^2$, to the objective function:

$$\text{R-FOP}(\theta^*, u) := \max_{x \in \mathcal{X}(u)} \{h(\theta^*; u)^\top x - \lambda \Omega(x)\}. \quad (11)$$

Here $\lambda > 0$ is the regularization coefficient. The objective $\{h(\theta^*; u)^\top x - \lambda \Omega(x)\}$ is strongly-concave in decision x , and the optimal solution is therefore unique:

$$x_\lambda^*(\theta^*; u) := \arg \max_{x \in \mathcal{X}(u)} \{h(\theta^*; u)^\top x - \lambda \Omega(x)\}. \quad (12)$$

We next show the regularized optimization is well-behaved.

PROPOSITION 1 (Properties of R-FOP). *Fix the context u . (1) **Unique Solution:** for any given parameter θ and regularization parameter $\lambda > 0$, the optimal solution of R-FOP(θ, u) defined in Equation (12) is unique. (2) **Lipschitz in parameter:** for fixed regularization parameter $\lambda > 0$, if $h(\theta; u)$ is L -Lipschitz in θ for any context u , then $x_\lambda^*(\theta; u)$ is $\frac{L}{\lambda}$ -Lipschitz with respect to θ . (3) **Convergence:** for any $\theta \in \Theta$, we have $x_\lambda^*(\theta; u) \rightarrow x^*(\theta; u)$ as $\lambda \rightarrow 0$.*

Proposition 1 suggests that the optimal solution of R-FOP is Lipschitz continuous in parameter θ , and when $\lambda \rightarrow 0$, the optimal regularized solution $x_\lambda^*(\theta; u)$ also converges to the optimal unregularized solution $x^*(\theta; u)$ of FOP in Equation (1). Accordingly, when λ is small, the regularized FOP provides a good approximation for the original FOP.

We now consider the suboptimality loss for the R-FOP with regularization parameter $\lambda > 0$, which maintains the convexity and smoothness of regularized objective in Equation (11) with respect to θ . Define $V_\lambda(\theta; u, x) := h(\theta; u)^\top x - \lambda \Omega(x)$ as the value function of the regularized optimization in Equation (11). The suboptimality loss associated with R-FOP(θ, u) is

$$L_\lambda(\theta; u, y) := \max_{x \in \mathcal{X}(u)} V_\lambda(\theta; u, x) - V_\lambda(\theta; u, y). \quad (13)$$

When $\lambda = 0$, $L_\lambda(\theta; u, y)$ reduces to the suboptimality loss in Equation (9).

Notably, the $L_\lambda(\theta; u, y)$ is precisely the Fenchel-Young (FY) loss defined on the region $\mathcal{X}(u)$ with observed decision y and the regularizer $\lambda\Omega$ (Blondel et al. 2020, 2022). The FY loss was originally introduced for structured prediction (SP) tasks, which often involved implementing arg max or rank on a score function over a simplex constraint to generate the prediction. The inverse optimization therefore generalizes the SP tasks, as arg max and rank over simplex constraints therein can be formulated as linear optimization with convex constraints. Thus, our work extends the FY loss beyond SP to IOP.

3.2. Statistical Property of Fenchel-Young Loss

In Section 2, we show that the excess distance risk $R_{\text{DIST}}(\theta) - \inf_\theta R_{\text{DIST}}(\theta)$ is indeed equivalent to the decision error $D(\theta, \theta^*)$. By adapting the result from Blondel et al. (2022, Proposition 3), we now establish the connection between the excess Fenchel-Young risk $R_\lambda(\theta) - \inf_\theta R_\lambda(\theta)$ and $D(\theta, \theta^*)$ in this part.

THEOREM 1 (Calibration Bound). *Suppose Assumptions 1 and 2 hold, and Ω is 1-strongly convex. We have, for any $\lambda > 0$ and $\theta \in \mathbb{R}^p$,*

$$D(\theta, \theta^*) = R(\theta) - R(\theta^*) \leq 2\mathbb{E}[\|x_\lambda^*(\theta; U) - x^*(\theta; U)\|_2^2] + \frac{4}{\lambda} [R_\lambda(\theta) - \inf_\theta R_\lambda(\theta)].$$

The term $\mathbb{E}[\|x_\lambda^*(\theta; U) - x^*(\theta; U)\|_2^2]$, represents the *regularization error* induced by coefficient λ for fixed θ , and it vanishes as $\lambda \rightarrow 0$ according to Proposition 1 property (3). We discuss the control of regularization error and the excess FY risk in Section 4.

The key insight of Theorem 1 is that, when λ is small, the excess FY risk $R_\lambda(\theta; u) - \inf_\theta R_\lambda(\theta; u)$ approximately provides an upper bound for the excess distance risk $R(\theta) - R(\theta^*)$. Therefore, the Fenchel-Young loss $L_\lambda(\theta; u, y)$ can be viewed as a convex and smooth **approximate surrogate loss** for the distance loss $L_{\text{DIST}}(\theta; u, y)$ introduced by Aswani et al. (2018). Therefore, minimizing the Fenchel-Young risk

$$\min_{\theta \in \Theta} R_\lambda(\theta) := \mathbb{E}[L_\lambda(\theta; U, Y)]$$

leads to approximate minimization of the decision error $D(\theta, \theta^*)$, and therefore may provide a reasonable approximation of the unknown true parameter θ^* of FOP in Equation (1).

3.3. Empirical Risk Minimization with Fenchel-Young Loss

In this part, we concretely discuss the properties FY loss following Blondel et al. (2020, 2022), which lay the foundation for designing a stochastic gradient descent (SGD) algorithm for minimizing the empirical Fenchel-Young risk:

$$\hat{\theta}_\lambda \leftarrow \min_{\theta \in \Theta} \hat{R}_\lambda(\theta) := \frac{1}{n} \sum_{i=1}^n L_\lambda(\theta; U_i, Y_i). \quad (14)$$

Algorithm 1 Inverse Optimization with FY Loss (SGD)

Require: Noisy data $\{(U_i, Y_i)\}_{i=1}^n$, learning rate $\eta > 0$, batch size m , maximum iteration $T > 0$, tolerance $\epsilon > 0$ and parameter space $\Theta \subseteq \mathbb{R}^p$.

- 1: Initialize parameter $\theta^{(0)} \in \Theta$.
- 2: **for** $t = 0, 1, \dots, T$ **do**
- 3: Sample a batch \mathcal{B}_t with size m from $\{(U_i, Y_i)\}_{i=1}^n$.
- 4: Compute the optimal solution $x_\lambda^*(\theta^{(t)}; U_i), i \in \mathcal{B}_t$.
- 5: Compute the batch-gradient of the empirical FY risk:

$$\nabla_\theta \widehat{R}_\lambda^{(t)} = \frac{1}{|\mathcal{B}_t|} \sum_{i \in \mathcal{B}_t} \left[\frac{\partial h(\theta; U_i)}{\partial \theta} \right]^\top (x_\lambda^*(\theta^{(t)}; U_i) - Y_i).$$

- 6: Update the parameter using the gradient-descent:

$$\theta^{(t+1)} = \theta^{(t)} - \eta \nabla_\theta \widehat{R}_\lambda^{(t)}.$$

- 7: **if** $\|\nabla_\theta \widehat{R}_\lambda^{(t)}\| \leq \epsilon$ **then**
- 8: **break.**
- 9: **end if**

10: **end for**

11: Return the estimated parameter $\hat{\theta}_\lambda \leftarrow \theta^{(T)}$.

Blondel et al. (2020, 2022) show that the Fenchel-Young loss $L_\lambda(\theta; u, y)$ is convex with respect to the parameter θ and admits a gradient under Assumption 3, enabling the use of SGD.

PROPOSITION 2 (Blondel et al. (2022), Proposition 3). *Suppose Assumption 3 holds. Fix $u \in \mathbb{R}^m$, $y \in \mathbb{R}^d$ and $\lambda > 0$. (1) **Continuity:** $L_\lambda(\theta; u, y)$ is continuous in θ for any given u and y , if the cost function $h(\theta; u)$ is continuous in θ for each given u . (2) **Convexity:** $L_\lambda(\theta; u, y)$ is convex in θ for any given u and y . (3) **Gradient:** By Danskin's theorem, we have $\nabla_\theta L_\lambda(\theta; u, y) = \left(\frac{\partial h(\theta; u)}{\partial \theta}\right)^\top (x_\lambda^*(\theta; u) - y)$, where $\frac{\partial h(\theta; u)}{\partial \theta}$ is the Jacobian matrix of h .*

Proposition 2 is crucial for applying the SGD for solving the empirical Fenchel-Young risk $\widehat{R}(\theta)$ in Equation (14). The convexity of Fenchel-Young loss $L_\lambda(\theta; u_i, Y_i)$ with respect to θ leads to the convexity of empirical Fenchel-Young risk $\widehat{R}(\theta)$, as the non-negative sample averaging of convex functions is still convex (Boyd 2004). The gradient of the empirical Fenchel-Young risk can be efficiently computed as the batch average of the gradients of the Fenchel-Young loss in each data point (Y_i, U_i) . We show the empirical FY risk minimization in Algorithm 1.

4. Theoretical Analysis

In this section, we analyze the expected decision error $D(\hat{\theta}_\lambda, \theta^*)$ induced by the estimated parameter $\hat{\theta}_\lambda$ from Algorithm 1. We then provide theoretical guarantees for the regret $\text{Reg}(\hat{\theta}_\lambda, \theta^*)$ and the parameter error $E(\hat{\theta}_\lambda, \theta) := \|\hat{\theta}_\lambda - \theta^*\|_1$. Detailed proofs are provided in Section EC.3. Before we proceed to the analysis, we first make the following assumption for the parameter space Θ in Algorithm 1.

ASSUMPTION 4 (Restricted Parameter Space). *Suppose the parameter space $\Theta \subseteq \mathbb{R}^d$ satisfies that, (1) **Lower Bounded Norm:** for fixed context $u \in \mathbb{R}^m$, the norm of cost function $h(\theta; u)$ is lower bounded by a positive constant, say $b(u) > 0$, i.e., $\|h(\theta; u)\|_2 \geq b(u)$ for all $\theta \in \Theta$. (2) **Well-Specification:** for fixed context $u \in \mathbb{R}^m$, the parameter space Θ contains a parameter $\theta_\lambda^*(u)$ such that $x_\lambda^*(\theta_\lambda^*(u); u) = \mathbb{E}[Y | u]$.*

Assumption 4 could be a strong assumption. We provide some examples to illustrate the assumption in Section EC.3.

4.1. Decision Error

In this section, we provide a modified calibration bound for the expected decision error $D(\hat{\theta}_\lambda, \theta)$ under Assumption 4, extending Theorem 1. The key difference is that, the excess FY risk $R_\lambda(\theta) - \inf_{\theta \in \Theta} R_\lambda(\theta)$ is now evaluated on the restricted parameter space Θ .

THEOREM 2 (Restricted Calibration Bound). *Suppose Assumptions 1, 2 and 4 hold. The function Ω is 1-strongly convex. For any $\lambda > 0$ and $\theta \in \Theta$, we have*

$$D(\theta, \theta^*) = R(\theta) - R(\theta^*) \leq \underbrace{2\mathbb{E}[\|x_\lambda^*(\theta; U) - x^*(\theta; U)\|_2^2]}_{\text{Regularization Error}} + \frac{4}{\lambda} \underbrace{[R_\lambda(\theta) - \inf_{\theta \in \Theta} R_\lambda(\theta)]}_{\text{Excess FY Risk}}.$$

Regularization Error For each fixed $\theta \in \Theta$, the regularization error measures the average distance of the regularized decision $x_\lambda^*(\theta; U)$ and the unregularized decision $x^*(\theta; U)$. We have shown in Proposition 1 that $\lambda \rightarrow 0$, the expected regularization error vanishes. This suffices for establishing the consistency in the expected decision error.

If we hope to establish non-asymptotic error bound, we need to further characterize how the regularization error $\mathbb{E}[\|x_\lambda^*(\theta; U) - x^*(\theta; U)\|_2^2]$ scales with the regularization coefficient λ . This requires analyzing the specific structure of the FOP, especially its feasible region $\mathcal{X}(u)$. In the following, we restrict our discussion to a special case, where the FOP is constrained in a ball that contains the origin, and the regularization function is $\Omega(x) = 1/2\|x\|_2^2$. We leave the general case for future work.

THEOREM 3 (Lipschitzness of Regularized Solution under Ball Constraint). Fix context $u \in \mathbb{R}^m$ and parameter $\theta \in \mathbb{R}^p$. Suppose the feasible set $\mathcal{X}(u) := \{x \in \mathbb{R}^d \mid \|x\|_2 \leq a(u)\}$ is a ball constraint with radius $a(u) > 0$, and the regularization function is $\Omega(x) = 1/2\|x\|_2^2$. If the critic value $\lambda_c(\theta; u) := \|h(\theta; u)\|/a(u)$ is positive, we then have

$$\begin{cases} \|x_\lambda^*(\theta; u) - x^*(\theta; u)\|_2 = 0, & 0 \leq \lambda \leq \lambda_c(\theta; u), \\ \|x_\lambda^*(\theta; u) - x^*(\theta; u)\|_2 \leq \lambda \frac{a(u)^2}{2\|h(\theta; u)\|_2}, & \lambda > \lambda_c(\theta; u). \end{cases}$$

Theorem 3 is essential to establish the bound of the regularization error for a fixed parameter $\theta \in \Theta$. However, the empirical minimizer $\hat{\theta}_\lambda \in \Theta$ depends on data and is therefore random. By assuming Assumption 4, we can establish the uniform bound over Θ :

$$\mathbb{E}[\|x_\lambda^*(\hat{\theta}_\lambda; U) - x^*(\hat{\theta}_\lambda; U)\|_2^2] \leq \lambda^2 \mathbb{E}[a(U)^4 / (4b(U)^2)]. \quad (15)$$

Therefore, as $\lambda \rightarrow 0$, the regularization error goes to zero, which confirms the result in Proposition 1.

Excess Fenchel-Young Risk To provide the generalization error bound for the excess Fenchel-Young risk $R_\lambda(\theta) - \inf_{\theta \in \Theta} R_\lambda(\theta)$, we introduce the empirical Rademacher complexity $\widehat{\mathcal{R}}_\lambda(\Theta)$ as

$$\widehat{\mathcal{R}}_\lambda(\Theta) := \mathbb{E}_\sigma \left[\sup_{\theta \in \Theta} \frac{1}{n} \sum_{i=1}^n \sigma_i \tilde{L}_\lambda(\theta; U_i, Y_i) \right].$$

Here $\tilde{L}(\theta; U_i, Y_i) := L_\lambda(\theta; U_i, Y_i) - \mathbb{E}[L_\lambda(\theta; U_i, Y_i)]$ is a centered Fenchel-Young loss, and $\sigma = \{\sigma_1, \dots, \sigma_n\}$ is a Rademacher sequence. The empirical Rademacher complexity $\widehat{\mathcal{R}}_\lambda(\Theta)$ measures the complexity of the parameter space Θ with respect to the empirical FY loss. By applying the empirical process theory, we can derive the following generalization bound for the excess FY risk.

LEMMA 2 (Symmetrization Bound, Wainwright (2019) - Theorem 4.10). Suppose that the parameter space Θ is bounded. Then for every finite u and y , the FY loss $L_\lambda(\theta; u, y)$ is also uniformly bounded over Θ by some constant (denoted by c). For any $\lambda > 0$, we have, with probability at least $1 - \delta$, $R_\lambda(\hat{\theta}_\lambda) - \inf_{\theta \in \Theta} R_\lambda(\theta) \leq 2\widehat{\mathcal{R}}_\lambda(\Theta) + \sqrt{\frac{2c^2 \log(1/\delta)}{n}}$.

In the statistical learning theory literature, there are standard approaches to bound the empirical Rademacher complexity for many common function classes. The empirical Rademacher complexity often goes to zero as the sample size n increases. We refer to Section EC.3.1.2 and Shalev-Shwartz and Ben-David (2014), Mohri (2018) for more details.

Decision Error Bound Suppose Assumptions 1, 3 and 4 hold. If the feasible region $\mathcal{X}(u)$ in Equation (11) is a ball-constrained region, we can establish the finite-sample bound for the expected decision error $D(\hat{\theta}_\lambda, \theta^*)$. Combining Theorems 2 and 3 and Lemma 2, we have

$$D(\hat{\theta}_\lambda, \theta^*) \leq \frac{\lambda^2 \mathbb{E}[a(U)^4]}{4b^2} + \frac{4}{\lambda} \left[\widehat{\mathcal{R}}_\lambda(\Theta) + \sqrt{\frac{c^2 \log(1/\delta)}{n}} \right].$$

We may further optimize the right-hand side of inequality with respect to $\lambda > 0$ to get a tighter bound on the decision error.

Table 1 Overview of the Synthetic Data Experiments.

Experiments	Forward Optimization Problem
Example A	$\min\{(\theta + u)^\top x \mid x \succeq 0, \ x\ _1 \leq a\}$
Example B	$\min\{(\theta \circ u)^\top x \mid x \in [-1, 1]^p\}$
Example C	$\min\{(\theta + u)^\top x \mid x \in [-1, 1]^p\}$
Example D	$\min\{x^\top x - (\theta + u)^\top x \mid x \in [0, 1]^p\}$
Example E	$\min\{-(\theta + u)^\top x \mid \ x\ _2 \leq a\}$

4.2. Decision Regret and Parameter Error

In this part, we show that the theoretical guarantees for the decision error $D(\hat{\theta}, \theta^*)$ directly lead to guarantees for the decision regret and the parameter error.

Decision Regret With the Cauchy-Schwarz inequality, we establish the following bound for the decision regret $\text{Reg}(\hat{\theta}_\lambda, \theta^*)$ in terms of the decision error $D(\hat{\theta}_\lambda, \theta^*)$.

THEOREM 4 (Decision Regret Bound). *If the expected squared norm of the true cost function $h(\theta^*; U)$ is bounded by some constant, say $\mathbb{E}[\|h(\theta^*; U)\|_2^2] \leq B$, we have $\text{Reg}(\hat{\theta}_\lambda, \theta^*) \leq BD(\hat{\theta}_\lambda, \theta^*)$.*

Theorem 4 indicates that the convergence of decision error $D(\hat{\theta}_\lambda, \theta^*)$ implies the convergence of decision regret $\text{Reg}(\hat{\theta}_\lambda, \theta^*)$, and any bound for the decision error implies the corresponding bound for the decision regret.

Parameter Error By assuming the identifiability condition proposed in Aswani et al. (2018, IC Conditions), we analyze the convergence of parameter error $E(\hat{\theta}_\lambda, \theta^*)$ in terms of the convergence of decision error $D(\hat{\theta}_\lambda, \theta^*)$.

THEOREM 5 (Uniform Convergence of Parameter Error). *Suppose Assumption 2 holds, and for all $\theta \in \Theta \setminus \theta^*$, $\text{dist}(\mathcal{X}^*(\theta; u), \mathcal{X}^*(\theta^*; u)) > 0$. Then for any θ such that $x^*(\theta; u) \rightarrow_p x^*(\theta^*; u)$, we have $\theta \rightarrow_p \theta^*$.*

Theorem 5 establishes the statistical convergence of decision error $D(\hat{\theta}_\lambda, \theta^*)$ implies the statistical convergence of parameter error $E(\hat{\theta}_\lambda, \theta^*)$ to zero.

5. Experiments

We conducted a series of synthetic and real data experiments, and we briefly present some of the results in this section, with more details deferred to Section EC.4.

5.1. Synthetic Data Experiments

We design a total of five synthetic data experiments, which encompass a variety of scenarios including box constraints, half-space constraints, ball constraints, linear objective functions and nonlinear

Table 2 The experimental results for various methods under different metrics for **Example A** in the Noisy Decision setting, where the FOP is defined as $\min\{(\theta + u)^\top x \mid x \succeq 0, \|x\|_1 \leq a\}$. For the Fenchel-Young (FY) loss, we set $\lambda = 0.1$ and $\Omega(x) = 1/2\|x\|_2^2$.

Sample size	Parameter Error				Decision Error				Regret			
	FY	SPA	KKA	VIA	FY	SPA	KKA	VIA	FY	SPA	KKA	VIA
50	1.30	2.46	4.25	3.81	3.03	4.53	7.66	3.90	0.05	0.20	0.77	0.08
100	1.17	1.35	4.58	4.12	2.47	2.94	7.79	3.17	0.03	0.06	0.84	0.05
300	0.53	2.10	4.87	4.42	2.05	2.66	8.22	2.19	0.02	0.08	0.93	0.03
500	0.53	2.44	4.92	4.52	1.64	2.69	8.32	1.88	0.01	0.10	0.95	0.03
1000	0.38	2.59	4.96	4.56	1.33	2.64	8.40	1.60	0.01	0.11	0.96	0.03

Table 3 The experimental results for various methods under different metrics for **Example B** in the Noisy Decision setting, where the FOP is defined as $\min\{(\theta \circ u)^\top x \mid x \in [-1, 1]^p\} = \min\{\sum_{k=1}^p \theta_k u_k x_k \mid x \in [-1, 1]^p\}$. We set $\lambda = 0.1$ and $\Omega(x) = 1/2\|x\|_2^2$.

Sample size	Parameter Error				Decision Error				Regret			
	FY	SPA	KKA	VIA	FY	SPA	KKA	VIA	FY	SPA	KKA	VIA
50	2.76	5.50	5.50	5.50	0.00	19.99	19.99	0.00	0.00	2.75	2.75	0.00
100	2.42	5.50	5.50	5.50	0.00	19.99	19.99	0.00	0.00	2.76	2.76	0.00
300	2.25	5.50	5.50	5.50	0.00	20.00	20.00	0.00	0.00	2.75	2.75	0.00
500	2.27	5.50	5.50	5.50	0.00	20.01	20.01	0.00	0.00	2.76	2.76	0.00
1000	2.19	5.50	5.50	5.50	0.00	19.99	19.99	0.00	0.00	2.75	2.75	0.00

objective functions, as shown in Table 1. For evaluation, we report the computational time, parameter error, decision error, and regret. All the results are averaged over 100 experiment replications.

Considering different forms of noisy observations, we examine three distinct settings for each example: **Noisy Decision** in Assumption 1, **Noisy Objective** in Remark 1, and a **Noiseless** setting (the true optimal decision of FOP is observed). For the former two settings, standard normal noises are added to the decision observations and the optimization objectives respectively.

In this section, we present the results for Examples A and B in the Noisy Decision setting. Specifically, we compare our method with other benchmark methods discussed in Section 2.2. These methods include the SPA (Semi-parametric methods), KKA (KKT-Approximated Loss), and VIA (Variational Inequality Loss) discussed in Section 2.2. The results are shown in Table 2 and Table 3 respectively. Notably, both Example A and Example B involve linear optimization, for which the VIA loss suboptimality Loss is equivalent to suboptimality loss as discussed in Section 2.2. More experimental results for other settings are available in Section EC.4.1.

Results for Example A Our approach, leveraging the Fenchel-Young loss, demonstrates superior performance across key metrics, including parameter error, decision error, and regret. Notably, it achieves the lowest values for these metrics compared to other traditional inverse optimization methods. While most methods, with the exception of KKA, exhibit gradual convergence in decision

Table 4 The **Relative Regret Ratio** column reports percentages (e.g., 1.01 represents a regret ratio of 1.01%). The **Period** column indicates the dataset’s time span in years (e.g., 1.5 corresponds to one and a half years). The **Computational Time** column lists average running times in seconds (e.g., 6 means an average of 6 seconds). For the Fenchel-Young loss, we set $\lambda = 0.1$ and $\Omega(x) = 1/2\|x\|_2^2$.

Period (years)	Decision Error					Relative Regret Ratio (%)					Computing time (seconds)				
	FY	SPA	KKA	VIA	MOM	FY	SPA	KKA	VIA	MOM	FY	SP	KKA	VIA	MOM
0.5	2.06	6.80	5.41	10.72	3.58	1.01	29.51	8.30	34.51	4.87	6	120	66	59	438
1	2.00	6.72	6.61	11.77	4.09	0.97	29.55	12.39	41.51	4.96	8	287	152	107	647
1.5	1.97	6.77	7.09	7.33	4.66	0.94	29.50	12.81	30.95	4.21	9	513	242	185	901
2	1.89	6.78	7.07	7.17	4.64	0.84	29.28	12.40	30.41	3.26	11	839	281	256	1218

error and regret as the sample size increases, their performance in parameter recovery remains consistently suboptimal. Even worse, the KKA method fails to converge in all of these metrics.

Results for Example B The FY loss and VIA demonstrate the best performance, achieving zero decision error and regret even with small sample sizes. In contrast, the KKA and SPA methods perform poorly with non-vanishing errors. Notably, the parameters θ estimated by SPA, KKA, and VIA often converge toward zero, causing problem degeneracy. Among these methods, VIA happens to successfully recover the correct sign of each element in θ , hence achieving zero decision error and regret. However, their nearly zero estimates are not very meaningful.

As explained in Section EC.4.1.2, the degeneracy arises because, in the optimization models of KKA, VIA, and SPA, $\theta = \mathbf{0}$ coincidentally represents an optimal solution. To alleviate the degeneracy issue, we have also tried introducing various regularization constraints, such as constraining the sum of θ ’s elements or the first element of θ to a nonzero value. However, these modifications did not lead to significant improvements so we omit them for brevity.

Computational Time In most experiments, our method achieves the shortest computational time across all experiments with an order-of-magnitude improvement. More detailed results are available in the Section EC.4.1.6.

Regularization Parameter Our experiments demonstrate that a small value of $\lambda > 0$ is sufficient to achieve robust performance. As the sample size increases, reducing λ further tends to improve results. For sufficiently large sample sizes, cross-validation can be used to select the optimal regularization parameter. A detailed analysis of how the regularization parameter λ impacts the performance of the FY loss L_λ is provided in Section EC.4.1.7.

5.2. Real data Experiments

We conducted experiments using a real-world dataset from Uber Movement (<https://movement.uber.com>), focusing on 45 census tracts in downtown Los Angeles. This dataset includes average travel times between neighboring tracts across 93 edges for 2018 and 2019. To construct an inverse

optimization problem, we solve for a shortest path for each travel time observation in the dataset, which serves as the observed optimal solution Y . Accordingly, we consider a shortest path problem as the FOP.

In our experiment setting, the context vector $u \in \mathbb{R}^{12}$ includes features such as wind speed and visibility. The travel times vector for 93 edges is modeled as θu , where $\theta \in \mathbb{R}^{93 \times 12}$ is the unknown parameter matrix. The shortest path FOP is given by $\min_x \left\{ \sum_{k=1}^{93} (\theta_k u) x_k \mid Ax = b \right\}$, where θ_k is the k -th row of the parameter matrix θ and $Ax = b$ is the flow constraints with $A \in \mathbb{R}^{45 \times 93}$ and $b \in \mathbb{R}^{45}$. The IOP task is to estimate θ from observations of shortest path solutions. For more experiment setup details, please see Section EC.4.2. In our experiment. In this real-data experiment, we continue to compare the FY loss approach with the benchmarks described in Section 2.2. Additionally, we note that the Maximum Optimality Margin (MOM) method proposed by Sun et al. (2023) can also be applied in this setting, we also include it as a benchmark method for comparison. Readers interested in this method can refer to Section EC.1.3.

We divide the dataset into four time spans: half a year (920 points), one year (1825 points), one and a half years (2735 points), and two years (3640 points). For each case, 60% of the data is allocated for training and 40% for testing. This random split is repeated across 30 independent experimental trials. The metrics collected include computational time, decision error, and relative regret ratio², where the decision error and regret ratio are both calculated on the testing data. We summarize the experimental results in Table 4 as below.

Decision Error The FY loss method achieves the lowest decision error across all time spans, significantly outperforming baseline approaches. This demonstrates its consistent ability to identify paths closely aligned with the true optimal solution. The MOM method ranks second, delivering near-optimal paths but falling short of our method’s accuracy. In contrast, SPA, VIA, and KKA exhibit substantially larger deviations from the optimal path.

Regret Ratio Consistent with its decision error performance, our method again surpasses all competitors, producing path travel times that tightly converge to the theoretical optimum. MOM remains the best competitor, maintaining a relatively low regret ratio, albeit still significantly higher than our approach. In contrast, KKA, SPA and VIA perform poorly, achieving even larger regret ratios.

Computational Time Our method delivers superior computational efficiency, completing tasks in seconds compared to the minutes or hours required by other methods. Competing approaches

² The relative regret ratio quantifies the testing regret of each method relative to the clairvoyant shortest paths on the testing data, normalized by the average traveling time of the clairvoyant shortest paths.

(SPA, VIA, KKA, MOM) rely on solving data-intensive constrained optimization problems, where runtime scales fast with input size. In contrast, our framework leverages a finite sequence of gradient descent steps, paired with lightweight gradient computations, to achieve rapid convergence. This orders-of-magnitude speed advantage makes our method uniquely viable for data-driven IOP with large datasets.

6. Conclusion

In this paper, we build a connection between inverse optimization and the Fenchel-Young (FY) loss originally designed for structured prediction. We propose a FY loss approach to data-driven inverse optimization with an efficient gradient-based optimization algorithm and rigorous theoretical guarantees. We demonstrate that this approach significantly outperforms many existing data-driven inverse-optimization methods in extensive simulations and real-data experiments. We hope this paper provides a new perspective on both FY loss and inverse optimization, opening more future research on FY loss for inverse optimization.

References

- Ahuja RK, Orlin JB (2001) Inverse optimization. *Operations research* 49(5):771–783.
- Aswani A, Shen ZJ, Siddiq A (2018) Inverse optimization with noisy data. *Operations Research* 66(3):870–892.
- Aswani A, Shen ZJM, Siddiq A (2019) Data-driven incentive design in the medicare shared savings program. *Operations Research* 67(4):1002–1026.
- Bärmann A, Pokutta S, Schneider O (2017) Emulating the expert: Inverse optimization through online learning. *International Conference on Machine Learning*, 400–410 (PMLR).
- Berge C (1877) *Topological spaces: Including a treatment of multi-valued functions, vector spaces and convexity* (Oliver & Boyd).
- Bertsimas D, Gupta V, Paschalidis IC (2015) Data-driven estimation in equilibrium using inverse optimization. *Mathematical Programming* 153:595–633.
- Besbes O, Fonseca Y, Lobel I (2023) Contextual inverse optimization: Offline and online learning. *Operations Research* .
- Birge JR, Li X, Sun C (2022) Stochastic inverse optimization. Technical report, Working paper.
- Blondel M, Llinares-López F, Dadashi R, Hussenot L, Geist M (2022) Learning energy networks with generalized fenchel-young losses. *Advances in Neural Information Processing Systems* 35:12516–12528.
- Blondel M, Martins A, Niculae V (2019) Learning classifiers with fenchel-young losses: Generalized entropies, margins, and algorithms. *The 22nd International Conference on Artificial Intelligence and Statistics*, 606–615 (PMLR).
- Blondel M, Martins AF, Niculae V (2020) Learning with fenchel-young losses. *Journal of Machine Learning Research* 21(35):1–69.
- Boyd S (2004) Convex optimization. *Cambridge UP* .
- Chan TC, Craig T, Lee T, Sharpe MB (2014) Generalized inverse multiobjective optimization with application to cancer therapy. *Operations Research* 62(3):680–695.
- Chan TC, Lee T (2018) Trade-off preservation in inverse multi-objective convex optimization. *European Journal of Operational Research* 270(1):25–39.
- Chan TC, Lee T, Terekhov D (2019) Inverse optimization: Closed-form solutions, geometry, and goodness of fit. *Management Science* 65(3):1115–1135.
- Chan TC, Mahmood R, Zhu IY (2023) Inverse optimization: Theory and applications. *Operations Research* .
- Chen L, Chen Y, Langevin A (2021) An inverse optimization approach for a capacitated vehicle routing problem. *European Journal of Operational Research* 295(3):1087–1098.
- Dong C, Chen Y, Zeng B (2018) Generalized inverse optimization through online learning. *Advances in Neural Information Processing Systems* 31.

- Elmachtoub AN, Grigas P (2022) Smart “predict, then optimize”. *Management Science* 68(1):9–26.
- Fernández-Blanco R, Morales JM, Pineda S (2021a) Forecasting the price-response of a pool of buildings via homothetic inverse optimization. *Applied Energy* 290:116791.
- Fernández-Blanco R, Morales JM, Pineda S, Porrás Á (2021b) Inverse optimization with kernel regression: Application to the power forecasting and bidding of a fleet of electric vehicles. *Computers & Operations Research* 134:105405.
- Kallus N, Mao X (2023) Stochastic optimization forests. *Management Science* 69(4):1975–1994.
- Keshavarz A, Wang Y, Boyd S (2011) Imputing a convex objective function. *2011 IEEE international symposium on intelligent control*, 613–619 (IEEE).
- Li JYM (2021) Inverse optimization of convex risk functions. *Management Science* 67(11):7113–7141.
- Lin B, Delage E, Chan TC (2024) Conformal inverse optimization. *arXiv preprint arXiv:2402.01489* .
- Mohajerin Esfahani P, Shafieezadeh-Abadeh S, Hanasusanto GA, Kuhn D (2018) Data-driven inverse optimization with imperfect information. *Mathematical Programming* 167:191–234.
- Mohri M (2018) *Foundations of machine learning* (MIT press).
- Qi M, Grigas P, Shen ZJM (2023) Integrated conditional estimation-optimization. URL <https://arxiv.org/abs/2110.12351>.
- Saez-Gallego J, Morales JM (2017) Short-term forecasting of price-responsive loads using inverse optimization. *IEEE Transactions on Smart Grid* 9(5):4805–4814.
- Saez-Gallego J, Morales JM, Zugno M, Madsen H (2016) A data-driven bidding model for a cluster of price-responsive consumers of electricity. *IEEE Transactions on Power Systems* 31(6):5001–5011.
- Shalev-Shwartz S, Ben-David S (2014) *Understanding machine learning: From theory to algorithms* (Cambridge university press).
- Sun C, Liu S, Li X (2023) Maximum optimality margin: A unified approach for contextual linear programming and inverse linear programming. *International Conference on Machine Learning*, 32886–32912 (PMLR).
- Van der Vaart AW (2000) *Asymptotic statistics*, volume 3 (Cambridge university press).
- Wainwright MJ (2019) *High-dimensional statistics: A non-asymptotic viewpoint*, volume 48 (Cambridge University Press).
- Yu S, Wang H, Dong C (2023) Learning risk preferences from investment portfolios using inverse optimization. *Research in International Business and Finance* 64:101879.
- Zattoni Scroccaro P, van Beek P, Mohajerin Esfahani P, Atasoy B (2024) Inverse optimization for routing problems. *Transportation Science* .

EC.1. Supplementary for Section 2

EC.1.1. Some Examples of Linear Forward Optimization

EXAMPLE EC.1 (CONSUMER UTILITY MODELS). The consumer demand model are widely used in characterize the consumer utility in electricity market (Saez-Gallego et al. 2016, Saez-Gallego and Morales 2017, Fernández-Blanco et al. 2021a,b). For each time period t , the model can be formulated as:

$$\max_y \{u_t(\theta; y) - p_t y \mid l_t \leq y \leq r_t\}, \quad (\text{EC.1.1})$$

where y is the electricity consumption level, restricted by l_t and r_t , p_t is the price at time t , and θ is the unknown parameter that characterizes the consumer utility function $u_t(\theta; y)$. As summarized in Chan et al. (2023), the utility $u_t(\theta; y)$ can be chosen as a piecewise linear function in θ :

$$u_t(\theta; y) = \begin{cases} \theta_{1,t} y, & \text{if } y < s, \\ \theta_{1,t} y + \dots + \theta_{i,t} (y - (i-1)s), & \text{if } (i-1)s \leq y \leq is, 2 \leq i \leq d. \end{cases}$$

By letting $h(\theta_t; u) = \theta_t$, $\theta_t = (\theta_{1,t}, \dots, \theta_{d,t})^\top \in \mathbb{R}^d$, $\bar{y} = (y\mathbb{I}_{y < s}, \dots, y\mathbb{I}_{(d-1)s \leq y < s})^\top \in \mathbb{R}^d$, and $g(u, \bar{y}) = (l_t - y, y - r_t)^\top \in \mathbb{R}^2$, the FOP in Equation (1) exactly captures the consumer demand model in Equation (EC.1.1).

EXAMPLE EC.2 (VEHICLE ROUTING PROBLEM). Chen et al. (2021) consider a vehicle routing problem with limited capacity. The FOP is formulated as a mixed-integer linear optimization model, as summarized in Chan et al. (2023):

$$\min_{x,y} \{\theta^\top x \mid Ax + By \geq d, \pi \leq y \leq Q\mathbf{1}, x \in \{0, 1\}^p\}.$$

Here, the variables x and y represent the arc choices and the amount of goods each vehicle carries, respectively. The unknown parameter θ is the cost vector of the arcs. The problem is constrained by the vehicle capacity Q and flow balance constraints. In this example, the objective is bilinear in the parameter θ and decision x , and the constraint is convex, fitting our formulation in Equation (1).

EC.1.2. Proof of Lemma 1

Proof of Lemma 1 By Assumption 2, we have

$$R(\theta) = \mathbb{E}[\min_{x \in \mathcal{X}^*(\theta; u)} \|Y - x\|_2^2] = \mathbb{E}[\|Y - x^*(\theta; U)\|_2^2].$$

The excess risk is then

$$\begin{aligned} R(\theta) - R(\theta^*) &= \mathbb{E}[\|Y - x^*(\theta; U)\|_2^2 - \|Y - x^*(\theta^*; U)\|_2^2] \\ &= \mathbb{E}[\|x^*(\theta; U)\|_2^2] - \mathbb{E}[\|x^*(\theta^*; U)\|_2^2] + 2\mathbb{E}[\mathbb{E}[Y \mid U]^\top (x^*(\theta^*; U) - x^*(\theta; U))] \end{aligned}$$

By Assumption 1, we have $\mathbb{E}[Y | U] = x^*(\theta^*; U)$ almost surely. Therefore, the excess risk can be further simplified as

$$\begin{aligned} R(\theta) - R(\theta^*) &= \mathbb{E}[\|x^*(\theta; U)\|_2^2] - \mathbb{E}[\|x^*(\theta^*; U)\|_2^2] + 2\mathbb{E}[\|x^*(\theta^*; U)\|_2^2] - 2\mathbb{E}[x^*(\theta^*; U)^\top x^*(\theta; U)] \\ &= \mathbb{E}[\|x^*(\theta; U) - x^*(\theta^*; U)\|_2^2], \end{aligned}$$

where the expectation is taken over the marginal distribution of U . This completes the proof.

EC.1.3. Loss Functions for Data-driven Inverse Optimization

KKT-Approximated Loss Keshavarz et al. (2011) consider a noiseless decision setting and propose a loss function that measures the violation of the Karush-Kuhn-Tucker (KKT) conditions:

$$L_{\text{KKA}}(\theta; u, y) := \min_{\lambda \geq 0} \{L_{\text{ST}}(\theta; u, y, \lambda) + L_{\text{CS}}(u, y, \lambda)\},$$

where λ is the dual variable and the two loss functions corresponds to the *stationary condition* and *complementary slackness* as follow:

$$\begin{aligned} L_{\text{ST}}(\theta; u, y, \lambda) &:= \left\| h(\theta; u) + \sum_{j=1}^m \lambda_j \nabla_x g_j(x, u) \right\|_2, \\ L_{\text{CS}}(u, y, \lambda) &:= \left\| (\lambda_1 g_1(x, u), \dots, \lambda_m g_m(x, u)) \right\|_2. \end{aligned}$$

In our setting with noisy observations, minimizing the IOP risk with L_{KKA} is challenging, as the decision may be entirely infeasible and thus significantly violate the KKT conditions. The experiments in Section 5 show that the KKT loss is sensitive to noise and may not converge to a reasonable estimation even when the sample size is large.

Suboptimality Loss Chan et al. (2014), Chan and Lee (2018) study the inverse optimization of multi-objective linear programming with single observation by minimizing the absolute duality gap between the primal objective value induced by observed decision and the dual objective value induced by the parameter. Bärmann et al. (2017) consider the suboptimality loss in the online learning setting. Chan et al. (2019) extend this framework to single noisy observation and proposed a goodness-of-fit metric for IOP. They proposed to estimate the parameters by minimizing the average duality gap between the objective function of observed decisions and the dual optimal objective $v(\theta; \lambda_i, U_i)$ induced by the parameter:

$$\min_{\theta, \epsilon_i, \lambda_i \geq 0, i=1, \dots, n} \frac{1}{n} \sum_{i=1}^n \epsilon_i \text{ s.t. } v(\theta; \lambda_i, U_i) - h(\theta; U_i)^\top Y_i \leq \epsilon_i.$$

Chan et al. (2023) points out Equation (8) is equivalent to minimizing the empirical risk $\widehat{R}(\theta)$ in Equation (7) with the loss replaced by the suboptimality loss as follows:

$$L_{\text{SUB}}(\theta; u, y) := \max_{x \in \mathcal{X}(u)} h(\theta; u)^\top x - h(\theta; u)^\top y.$$

Although the optimization problem in this approach is convex and tractable, this duality-based approach still faces several challenges. (1) If there exists a parameter $\theta \in \Theta$ such that $h(\theta; u) = 0$, the suboptimality loss L_{SUB} also reaches zero, causing the inverse optimization problem to degenerate. (2) As the sample size and decision dimension increase, the existing dual formulation in Equation (8) for solving empirical risk induced by suboptimality loss becomes computationally challenging. (3) It is unknown that whether the empirical risk minimization with the suboptimality loss leads to the theoretical control for the decision error we target in Equation (4).

Variational Inequality Loss Inspiring by the *variational inequality*, Bertsimas et al. (2015) study the variational inequality approximation (VIA) loss function that measures the optimality margin for the FOP with a differentiable objective function $f(\theta; u, x)$:

$$\nabla_x f(\theta; u, x)^\top (x - x^*(\theta; u)) \geq 0,$$

where $f(\theta; u, x)$ is the objective function of the FOP. For an observed decision $y \in \mathbb{R}^d$, the VIA loss is defined as:

$$L_{\text{VIA}}(\theta; u, y) = \max_{x \in \mathcal{X}(u)} \nabla_y f(\theta; u, y)^\top (x - y).$$

As noted by Chan et al. (2023), for linear FOPs, the VIA loss is equivalent to the suboptimality loss in Equation (9), as:

$$L_{\text{VIA}}(\theta; u, y) = |\max_{x \in \mathcal{X}} h(\theta; u)^\top (x - y)| = L_{\text{SUB}}(\theta; u, y).$$

Bertsimas et al. (2015) propose solving the VIA loss via strong duality formulation, which facing the same computational challenges as the suboptimality loss. The VIA loss is also sensitive to noise, as observed decisions may fall outside the feasible region, leading to large VIA losses.

Distance Loss Aswani et al. (2018) propose an IOP algorithm that directly minimizes the expected decision error $E(\theta, \theta^*)$ over Θ in Equation (4) by considering minimized the squared distance disk as shown in Equation (2).

$$L_{\text{DIST}}(\theta; u, y) := \min_{x \in \mathcal{X}^*(\theta; u)} \|y - x\|_2^2.$$

By enforcing strong duality, Aswani et al. (2018) reformulate the empirical IOP risk with distance loss as a convex optimization problem:

$$\begin{aligned} \widehat{R}_{\text{DIST}}(\theta) &:= \min_{x_i, \lambda_i} \frac{1}{n} \sum_{i=1}^n \|Y_i - x_i\|_2^2 \\ \text{s.t. } &v(\theta; \lambda_i, U_i) - h(\theta; U_i)^\top x_i \leq 0, \quad \forall i \in [n] \\ &g(U_i, x_i) \leq 0, \quad \forall i \in [n] \\ &\lambda_i \geq 0, \quad \forall i \in [n]. \end{aligned}$$

Here, $v(\theta; \lambda_i, U_i)$ is the Lagrangian dual function of the FOP, and λ_i is the dual variable for each observed decision Y_i . Note that, even when Assumption 2 holds, directly minimizing the expected decision error $D(\theta, \theta^*)$ or the IOP risk $R(\theta)$ in Equation (2) over Θ presents significant challenges. The primary difficulty arises from the non-convexity of the objective function $\|x^*(\theta; U) - x^*(\theta^*)\|_2^2$, making it difficult to find the global minimum. In addition, $D(\theta, \theta^*)$ may not be continuous in θ , which means the subgradient $\partial_\theta D(\theta, \theta^*)$ may not exist, preventing the use of gradient-based optimization methods. To address this, Aswani et al. (2018) propose an enumeration algorithm that evaluates $R(\theta)$ over a discretized parameter space Θ . However, this approach becomes computationally expensive in high-dimensional settings. Moreover, computing $R(\theta)$ involves solving a convex optimization problem, whose complexity scales significantly with the sample size and decision dimension, further exacerbating computational challenges.

Semi-parametric Methods To overcome the limitations of squared distance loss with large problems, Aswani et al. (2018) proposed a semi-parametric (SPA) method that first uses the Nadaraya-Watson (NW) estimator to denoise the observed decisions and then projects them onto the feasible region, denoted as \tilde{X}_i . Aswani et al. (2018) then propose to solve Equation (8) by replacing Y_i with \tilde{X}_i for each $i \in [n]$, that is,

$$\begin{aligned} \min_{\theta, \epsilon_i, \lambda_i} \frac{1}{n} \sum_{i=1}^n \epsilon_i \quad \text{s.t.} \quad & v(\theta; \lambda_i, U_i) - h(\theta; U_i)^\top \tilde{X}_i \leq \epsilon_i, \\ & \theta \in \Theta, \quad \lambda_i \geq 0, \quad \forall i \in [n]. \end{aligned} \quad (\text{EC.1.2})$$

However, the NW estimator performs poorly with high-dimensional context space, and the dual formulation is also computationally expensive when the sample size and dimension grow. Meanwhile, such estimate-then-project approach separates the de-noising process from the structure of FOP, potentially resulting in suboptimal performance.

Maximum Optimality Margin Sun et al. (2023) considered an inverse optimization method for which the FOP is a linear program (LP). Specifically, they analyzed the following LP from the perspective of the simplex method, assuming that the observed solution $x^* = (x_1, \dots, x_n)^\top$ is noise-free.

$$\begin{aligned} \text{LP}(c, A, b) := \min \quad & c^\top x \\ \text{s.t.} \quad & Ax = b, x \geq 0 \end{aligned}$$

where $c \in \mathbb{R}^n$, $A \in \mathbb{R}^{m \times n}$, and $b \in \mathbb{R}^m$. Based on the simplex method, they define the optimal basis \mathcal{B}^* and its complement \mathcal{N}^* as follows,

$$\mathcal{B}^* := \{i : x_i^* > 0\}, \quad \mathcal{N}^* := \{i : x_i^* = 0\}.$$

For a set $\mathcal{B} \subset [n]$, they use $A_{\mathcal{B}}$ to denote the submatrix of A with column indices corresponding to \mathcal{B} and $c_{\mathcal{B}}$ to denote the subvector with corresponding dimensions. Therefore, we have $\mathcal{B} = \mathcal{B}^*$ if and only if

$$c_{\mathcal{N}}^\top - c_{\mathcal{B}}^\top A_{\mathcal{B}}^{-1} A_{\mathcal{N}} \geq 0 \quad (\text{EC.1.3})$$

Suppose there is a linear mapping from the covariates z_t to the objective vector c_t , i.e., $g(z_t; \Theta) := \Theta z_t$. The Maximum Optimality Margin (MOM) method solves the following optimization problem.

$$\begin{aligned} \hat{\Theta} := \arg \min_{\Theta \in \mathcal{K}} \quad & \frac{\lambda}{2} \|\Theta\|_2^2 + \frac{1}{T} \sum_{t=1}^T \|s_t\|_1 \\ \text{s.t.} \quad & \hat{c}_t = \Theta z_t, \quad t = 1, \dots, T, \\ & \hat{c}_{t, \mathcal{N}_t^*}^\top - \hat{c}_{t, \mathcal{B}_t^*}^\top A_{t, \mathcal{B}_t^*}^{-1} A_{t, \mathcal{N}_t^*} \geq 1_{|\mathcal{N}_t^*|} - s_t, \quad t = 1, \dots, T. \end{aligned}$$

where the decision variables are $\Theta \in \mathbb{R}^{n \times d}$, $\hat{c}_t \in \mathbb{R}^n$, and $s_t \in \mathbb{R}^{|\mathcal{N}_t|}$. Furthermore, \mathcal{K} is a convex set to be determined. This optimization problem essentially characterizes the extent to which the optimality condition Equation (EC.1.3) is satisfied, that is, it aims to achieve the largest possible margin for satisfying the inequality constraints. However, the MOM method is invalid when the observed solution is not at a vertex of the convex feasible region (for example, in the Noisy Decision setting, the observed decision is not even feasible), and therefore the basis of the observed solution cannot be identified.

EC.2. Supplementary for Section 3

EC.2.1. Proof of Proposition 1

Proof of Proposition 1 The proof is as follow.

- **Uniqueness of Optimal Solution:** For fixed parameter θ , context u and regularization parameter $\lambda > 0$, the objective function $h(\theta; u)^\top x - \lambda\Omega(x)$ is strongly concave in x . Meanwhile the feasible region $\mathcal{X}(u)$ is also convex. Therefore, for every fixed θ , u and $\lambda > 0$, the regularized FOP defined in Equation (12) is a strongly convex problem, which implies the uniqueness of the optimal solution $x_\lambda^*(\theta; u)$.

- **Lipschitzness of Regularized Solution in Parameter θ :** For the Lipschitz continuity of regularized solution $x_\lambda^*(\theta; u)$ with respect to θ , we follows the proof of Proposition 2 in Qi et al. (2023). Note that, if a function F is γ -strongly convex over \mathbb{R}^d with respect to the Euclidean norm $\|\cdot\|_2$, then we have

$$F(y) - F(x) - \nabla F(x)^\top (y - x) \geq \frac{\gamma}{2} \|y - x\|_2^2.$$

Let $x^* = \arg \min_{x \in \mathbb{R}^d} F(x)$ be the minimizer of function F over \mathbb{R}^d , and the optimality condition suggests that

$$\nabla F(x^*)^\top (y - x^*) \geq 0$$

for any $y \in \mathbb{R}^d$. Therefore, we have

$$F(y) - F(x^*) \geq \frac{\gamma}{2} \|y - x^*\|_2^2. \quad (\text{EC.2.1})$$

Now, for fixed context u , consider the function $F_\theta(x) = \lambda\Omega(x) - h(\theta; u)^\top x$, which is λ -strongly convex. By the definition of regularized decision in Equation (EC.3.5), we have

$$x_\lambda^*(\theta; u) := \arg \max_{x \in \mathcal{X}(u)} \left\{ h(\theta; u)^\top x - \lambda\Omega(x) \right\} = \arg \min_{x \in \mathcal{X}(u)} F_\theta(x).$$

Applying Equation (EC.2.1), for any $\theta, \theta' \in \mathbb{R}^p$, we have

$$F_\theta(x_\lambda^*(\theta'; u)) - F_\theta(x_\lambda^*(\theta; u)) \geq \frac{\lambda}{2} \|x_\lambda^*(\theta'; u) - x_\lambda^*(\theta; u)\|_2^2.$$

Switching the role of θ and θ' , we have

$$F_{\theta'}(x_\lambda^*(\theta; u)) - F_{\theta'}(x_\lambda^*(\theta'; u)) \geq \frac{\lambda}{2} \|x_\lambda^*(\theta; u) - x_\lambda^*(\theta'; u)\|_2^2.$$

Adding the above two inequalities together, we have

$$\begin{aligned}
\lambda \|x_\lambda^*(\theta'; u) - x_\lambda^*(\theta; u)\|_2^2 &\leq F_\theta(x_\lambda^*(\theta'; u)) - F_\theta(x_\lambda^*(\theta; u)) + F_{\theta'}(x_\lambda^*(\theta; u)) - F_{\theta'}(x_\lambda^*(\theta'; u)) \\
&= [F_\theta(x_\lambda^*(\theta'; u)) - F_{\theta'}(x_\lambda^*(\theta'; u))] - [F_\theta(x_\lambda^*(\theta; u)) - F_{\theta'}(x_\lambda^*(\theta; u))] \\
&= [(h(\theta'; u) - h(\theta; u))^\top x_\lambda^*(\theta'; u)] - [(h(\theta'; u) - h(\theta; u))^\top x_\lambda^*(\theta; u)] \\
&= (h(\theta'; u) - h(\theta; u))^\top [x_\lambda^*(\theta'; u) - x_\lambda^*(\theta; u)] \\
&\leq \|h(\theta'; u) - h(\theta; u)\|_2 \cdot \|x_\lambda^*(\theta'; u) - x_\lambda^*(\theta; u)\|_2 \\
&\leq L \|\theta' - \theta\|_2 \cdot \|x_\lambda^*(\theta'; u) - x_\lambda^*(\theta; u)\|_2.
\end{aligned}$$

The first inequality is established by the strong convexity of $F_\theta(x)$ with respect to x , while the second inequality follows from the Cauchy-Schwarz inequality. The last inequality follows from the Lipschitz continuity of $h(\theta; u)$ with respect to θ . Dividing both sides by $\|x_\lambda^*(\theta'; u) - x_\lambda^*(\theta; u)\|_2$, we have

$$\|x_\lambda^*(\theta'; u) - x_\lambda^*(\theta; u)\|_2 \leq \frac{1}{\lambda} \|\theta' - \theta\|_2.$$

• **Uniform Convergence of Regularized Solution in Regularization Parameter λ :** We adapt this proof from Qi et al. (2023). When the parameter θ and the context u are all fixed, the optimal regularized decision $x_\lambda^*(\theta; u)$ can be viewed as a function that maps the regularization parameter $\lambda > 0$ to the feasible set $\mathcal{X}(u)$. To simplify the notations, we denote $x_\lambda^*(\theta; u)$ as x_λ^* and $x^*(\theta; u)$ as x^* .

Given the sequence $\{\lambda_n > 0\}$ that converges to zero when $n \rightarrow \infty$, we define a corresponding sequence $\{x_{\lambda_n}^*\}$. If $\|x_{\lambda_n}^* - x^*\|_2 \not\rightarrow 0$ as $n \rightarrow \infty$, there exists a subsequence $\{x_{\lambda_{n_k}}^*\}$ such that $\|x_{\lambda_{n_k}}^* - x^*\|_2 \geq \epsilon$ for some $\epsilon > 0$. By the compactness of the feasible set $\mathcal{X}(u)$, the subsequence $\{x_{\lambda_{n_k}}^*\}$ converges to a limit point $x_\infty^* \in \mathcal{X}(u)$ as $k \rightarrow \infty$.

Due to the continuity of the objective function in Equation (11) with respect to λ , the Maximum theorem (Berge 1877) guarantees that the optimal regularized solution x_n^* is upper hemicontinuous with respect to the regularization parameter λ . Since $\lambda_{n_k} \rightarrow 0$ as $k \rightarrow \infty$, we have $x_\infty^* = x^*$ by the definition of upper hemicontinuous. This implies that the $\lim_{n \rightarrow \infty} x_{\lambda_n}^* = x^*$, which contradicts the assumption that $\|x_{\lambda_n}^* - x^*\|_2 \not\rightarrow 0$ as $n \rightarrow \infty$. We then complete the proof.

EC.2.2. Proofs of Theorem 1

First notice that the expected decision error $D(\theta, \theta^*)$ can be upper bounded by

$$D(\theta, \theta^*) = \mathbb{E}[\|x^*(\theta; U) - x^*(\theta^*; U)\|_2^2] \leq 2\mathbb{E}\|x^*(\theta; U) - x_\lambda^*(\theta; U)\|_2^2 + 2\mathbb{E}\|x_\lambda^*(\theta; U) - x^*(\theta^*; U)\|_2^2. \quad (\text{EC.2.2})$$

By Lemma 1, the excess distance risk $R(\theta) - R(\theta^*)$ is equivalent to the expected decision error $D(\theta, \theta^*)$. Therefore, it is sufficient to provide an upper bound of $D(\theta, \theta^*)$ in terms of the the excess FY risk $R_\lambda(\theta) - \inf_\theta R_\lambda(\theta)$.

To begin with, we define the conditional Fenchel-Young risk as follow:

$$\begin{aligned}
\mathcal{R}_\lambda(\theta; u) &= \mathbb{E}[L_\lambda(\theta; U, Y) | u] \\
&= \mathbb{E}[V_\lambda^*(\theta; U) | u] + \lambda \mathbb{E}[\Omega(Y) | u] - h(\theta; u)^\top \mathbb{E}[Y | u] \\
&= V_\lambda^*(\theta; u) + \lambda \Omega(\mathbb{E}[Y | u]) - h(\theta; u)^\top \mathbb{E}[Y | u] + \lambda (\mathbb{E}[\Omega(Y) | u] - \Omega(\mathbb{E}[Y | u])) \\
&= L_\lambda(\theta; u, \mathbb{E}[Y | u]) + \lambda (\mathbb{E}[\Omega(Y) | u] - \Omega(\mathbb{E}[Y | u])).
\end{aligned} \tag{EC.2.3}$$

Note that $\mathbb{E}[Y | u]$ is the expected decision under the context u , which is exactly the optimal (noiseless) decision $x^*(\theta^*; u)$ as we assumed in Assumption 1. Meanwhile, $\mathbb{E}[\Omega(Y) | u] - \Omega(\mathbb{E}[Y | u])$ is known as *Jensen's gap*, which is non-negative due to the convexity of Ω .

Due to the zero loss property of $L_\lambda(\theta; u, \mathbb{E}[Y | u])$ as shown in Proposition 2, we have

$$\inf_{\theta} \mathcal{R}_\lambda(\theta; u) = \lambda (\mathbb{E}[\Omega(Y) | u] - \Omega(\mathbb{E}[Y | u])) \tag{EC.2.4}$$

and the conditional excess FY risk then takes the form

$$\mathcal{R}_\lambda(\theta; u) - \inf_{\theta} \mathcal{R}_\lambda(\theta; u) = L_\lambda(\theta; u, \mathbb{E}[Y | u]). \tag{EC.2.5}$$

As we mentioned at the beginning of Section 3, the regularization function Ω is strongly convex. Therefore the Fenchel-Young loss $L_\lambda(\theta; u, \mathbb{E}[Y | u])$ is also strongly convex in θ for each fixed context u . We are now ready to establish the calibration bound in Theorem 1.

Proof of Theorem 1 If a function F is γ -strongly convex over \mathcal{C} with respect to the Euclidean norm $\|\cdot\|_2$, then we have

$$F(y) - F(x) - \nabla f(x)^\top (y - x) \geq \frac{\gamma}{2} \|y - x\|_2^2.$$

If \mathcal{C} is a closed convex set, the minimizer $x^* = \arg \min_{x \in \mathcal{C}} F(x)$ of function F satisfies the optimality condition

$$\nabla f(x^*)^\top (y - x^*) \geq 0 \tag{EC.2.6}$$

for any $y \in \mathcal{C}$. Therefore, we have

$$F(y) - F(x^*) \geq \frac{\gamma}{2} \|y - x^*\|_2^2. \tag{EC.2.7}$$

Now, define the function $F(x) = \lambda \Omega(x) - h(\theta; u)^\top x$, which is λ -strongly convex. As we assume $\mathcal{X}(u)$ is closed and convex for each context u , the optimal regularized decision

$$x_\lambda^*(\theta; u) = \arg \max_{x \in \mathcal{X}(u)} \left\{ h(\theta; u)^\top x - \lambda \Omega(x) \right\} = \arg \min_{x \in \mathcal{X}(u)} \left\{ \lambda \Omega(x) - h(\theta; u)^\top x \right\} = \arg \min_{x \in \mathcal{X}(u)} F(x)$$

satisfies the optimality condition Equation (EC.2.6). According to Equation (EC.2.7), we have

$$\left(\lambda\Omega(y) - h(\theta; u)^\top y\right) - \left(\lambda\Omega(x_\lambda^*(h; u)) - h(\theta; u)^\top x_\lambda^*(\theta; u)\right) \geq \frac{\lambda}{2} \|y - x_\lambda^*(\theta; u)\|_2^2.$$

As we see, the LHS of above inequality is exactly the Fenchel-Young loss $L_\Omega(\theta; u, y)$, we then have

$$L_\lambda(h; u, y) \geq \frac{\lambda}{4} \|y - x_\lambda^*(h; u)\|_2^2.$$

By replacing y with the conditional expectation $\mathbb{E}[Y | u]$, we have

$$L_\lambda(h; u, \mathbb{E}[Y | u]) \geq \frac{\lambda}{4} \|\mathbb{E}[Y | u] - x_\lambda^*(h; u)\|_2^2.$$

Assumption 1 suggests that $\mathbb{E}[Y | u] = x^*(\theta^*; u)$, which is the optimal decision induced by the true parameter θ^* . Therefore, by combining with the result in Equation (EC.2.5), we have for any fixed context u ,

$$\frac{\lambda}{2} \|x^*(\theta^*; u) - x_\lambda^*(\theta; u)\|_2^2 \leq L_\lambda(\theta; u, \mathbb{E}[Y | u]) = R_\lambda(\theta; u) - \inf_\theta R_\lambda(\theta; u). \quad (\text{EC.2.8})$$

Taking the expectation on both sides of the inequality, we have

$$\mathbb{E}[\|x^*(\theta^*; U) - x_\lambda^*(\theta; U)\|_2^2] \leq \mathbb{E}[R_\lambda(\theta; U) - \inf_\theta R_\lambda(\theta; U)] = R_\lambda(\theta) - \inf_\theta R_\lambda(\theta).$$

Combining the result in Equation (EC.2.2) leads to the desired result.

EC.2.3. Proof of Proposition 2

Recall the Fenchel-Young loss introduced in Equation (13) takes the form

$$L_\lambda(\theta; u, y) = V_\lambda^*(\theta; u) + \lambda\Omega(y) - h(\theta; u)^\top y,$$

where the optimal value function $V_\lambda^*(\theta; u) := \max\{h(\theta; u)^\top x - \lambda\Omega(x)\}$ is known as the Fenchel-Moreau conjugate of the regularization function Ω . We first establish the properties of $V_\lambda^*(\theta; u)$, and then analyze the Fenchel-Young loss.

LEMMA EC.1 (Fenchel-Moreau Conjugate). *Fix context $u \in \mathbb{R}^m$ and regularization parameter $\lambda > 0$. (1) **Convexity:** If $h(\theta; u)$ is convex in θ , the Fenchel-Moreau conjugate $V_\lambda^*(\theta; u)$ is convex in θ . (2) **Continuity:** If $h(\theta; u)$ is continuous with respect to θ (for every fixed context u), the Fenchel-Moreau conjugate $V_\lambda^*(\theta; u)$ is also continuity with respect to θ . (3) **Gradient:** By the strongly convexity of Ω , the optimal decision $x_\lambda^*(\theta; u)$ is unique. If $h(\theta; u)$ is convex and differentiable in θ , by Danskin's theorem, we have*

$$\nabla_\theta V_\lambda^*(\theta; u) = \frac{\partial h(\theta; u)}{\partial \theta} x_\lambda^*(\theta; u).$$

Proof of Lemma EC.1 The proof is as follow.

1. **Convexity:** The objective function $h(\theta; u)^\top x$ represents a linear combination of the components of $h(\theta; u) \in \mathbb{R}^d$ weighted by the entries of x . Specifically, for each fixed $u \in \mathbb{R}^m$,

$$h(\theta; u)^\top x = \sum_{i=1}^d x_i h_i(\theta; u).$$

If the cost function $h(\theta; u)$ is convex in θ for each fixed u , a weighted sum of convex functions is still convex. Therefore, the objective function $h(\theta; u)^\top x$ is convex in θ for each fixed u .

Moreover, as $V_\lambda^*(\theta)$ is defined as the point-wise maximum of $h(\theta; u)^\top x$ over the bounded convex set $\mathcal{X}(u)$, which preserves the convexity of $h(\theta; u)^\top x$. Therefore, the Fenchel-Moreau conjugate $V_\lambda^*(\theta)$ is also convex in θ .

2. **Continuity:** If $h(\theta; u)$ is continuous with respect to θ for each fixed u , the Fenchel-Moreau conjugate $V_\lambda^*(\theta; u)$ is also continuous with respect to θ . This is guaranteed by the Berge Maximum Theorem (Berge 1877).

3. **Gradient:** As we mention previously, for each $x \in \mathcal{X}(u)$, if the cost function $h(\theta; u)$ is convex in θ , the objective $h(\theta; u)^\top x$ is convex in θ . By Danskin's theorem and the differentiability of $h(\theta; u)$ with respect to θ , we have

$$\nabla_\theta V_\lambda^*(\theta; u) = \nabla_\theta \{h(\theta; u)^\top x_\lambda^*(\theta; u)\} = \frac{\partial h(\theta; u)}{\partial \theta} x_\lambda^*(\theta; u).$$

Without the convexity assumption in θ , if $h(\theta; u)$ is continuously differentiable in θ for all $x \in \mathcal{X}(u)$, that is, the gradient $\nabla_\theta \{h(\theta; u)^\top x\}$ is continuous, such result is also established by Envelope theorem.

Proof of Proposition 2 We now establish the properties of FY loss based on Lemma EC.1 and Assumption 3.

1. **Zero loss:** Recall that the regularized optimal decision in Equation (12) is defined as

$$x_\lambda^*(\theta; u) = \max_{x \in \mathcal{X}(u)} V_\lambda(\theta; u, x).$$

If $x_\lambda^*(\theta; u) = y$, then we have $L_\lambda(\theta; u, y) = V_\lambda(\theta; u, x_\lambda^*(\theta; u)) - V_\lambda(\theta; u, y) = 0$. On the other hand, if $L_\lambda(\theta; u, y) = 0$, we have $V_\lambda(\theta; u, x_\lambda^*(\theta; u)) = V_\lambda(\theta; u, y)$. Since the maximum is unique by assumption, we then have $x_\lambda^*(\theta; u) = y$.

2. **Continuity:** If $h(\theta; u)$ is continuous with respect to θ for each fixed u , the Fenchel-Moreau conjugate $V_\lambda^*(\theta; u)$ is also continuous with respect to θ by Lemma EC.1. Therefore, the Fenchel-Young loss $L_\lambda(\theta; u, y)$ is continuous in θ for each fixed u and y .

3. **Gradient:** The gradient of Fenchel-Young loss can be derived directly from Lemma EC.1.

4. **Convexity:** By Assumption 3, $h(\theta; u)$ is linear in θ , and the Fenchel conjugate $V_\lambda^*(\theta; u)$ is still convex in θ . Therefore, the Fenchel-Young loss $L_\lambda(\theta; u, y)$ is convex in θ .

EC.3. Supplementary for Section 4

In this section, we analyze the upper bound for the expected decision error by providing the following modified calibration bound for $D(\hat{\theta}_\lambda, \theta)$ under Assumption 4. The key difference is that, the excess FY risk $R_\lambda(\theta) - \inf_{\theta \in \Theta} R_\lambda(\theta)$ is now evaluated on the space Θ instead of the \mathbb{R}^d space.

THEOREM EC.1 (Existence of Restricted Parameter Space). *Suppose Assumption 1 holds and $\Omega(x) = 1/2\|x\|_2^2$. Define \mathcal{U} as the support of context. For every fixed context u , if the objective function of FOP induced by the true parameter θ^* is lower bounded by some constant b , i.e., $h(\theta^*; u)^\top x^*(\theta^*; u) > b$, we can construct the following parameter space that satisfies Assumption 4:*

$$\Theta_\lambda = \{\theta_\lambda : h(\theta_\lambda; u) = h(\theta^*; u) + \lambda \mathbb{E}[Y | u], u \in \mathcal{U}\}.$$

Once the cost function $h(\theta; u)$ is determined, the restricted parameter space Θ_λ can be constructed based on the support of context \mathcal{U} . The following are some examples of constructing the restricted parameter space Θ_λ based on the form of cost function $h(\theta; u)$.

EXAMPLE EC.3 (ADDITIVE COST). Suppose $\theta \in \mathbb{R}^d$, $u \in \mathcal{U} \subseteq \mathbb{R}^d$ and we $h(\theta; u) = \theta + u$. By Assumption 1, we have $\mathbb{E}[Y | u] = x^*(\theta^*; u) \in \mathcal{X}(u) \subseteq \mathbb{R}^d$ for each context $u \in \mathcal{U}$. According to Theorem EC.1, we consider the following restricted parameter space $\Theta_\lambda = \{\theta_\lambda : \theta_\lambda = \theta^* + \lambda \mathbb{E}[Y | u], u \in \mathcal{U}\}$.

EXAMPLE EC.4 (MULTIPLY COST). Suppose $\theta \in \mathbb{R}^d$, $u \in \mathcal{U} \subseteq \mathbb{R}^d$ and we $h(\theta; u) = \theta * u$, where $*$ is element-wise multiplication of vector. By Assumption 1, we have $\mathbb{E}[Y | u] = x^*(\theta^*; u) \in \mathcal{X}(u) \subseteq \mathbb{R}^d$ for each context $u \in \mathcal{U}$. According to Theorem EC.1, we consider the following restricted parameter space $\Theta_\lambda = \{\theta_\lambda : \theta_\lambda = \theta^* + \lambda \frac{\mathbb{E}[Y|u]}{u}, u \in \mathcal{U}\}$.

Proof of Theorem EC.1 We fix the context $u \in \mathcal{U}$ in the following proof.

• **Lower Bounded Norm:** By Assumption 1, we have $x^*(\theta^*; u) = \mathbb{E}[Y | u]$. For any $\theta_\lambda \in \Theta_\lambda$, we then have

$$\begin{aligned} \|h(\theta_\lambda; u)\|_2^2 &= \|h(\theta^*; u) + \lambda \mathbb{E}[Y | u]\|_2^2 \\ &= \|h(\theta^*; u)\|_2^2 + 2\lambda h(\theta^*; u)^\top \mathbb{E}[Y | u] + \lambda^2 \|\mathbb{E}[Y | u]\|_2^2 \\ &\geq 2\lambda h(\theta^*; u)^\top \mathbb{E}[Y | u] \geq 2\lambda b. \end{aligned}$$

Therefore, we have for every $\theta \in \Theta_\lambda$, $\|h(\theta; u)\|_2 \geq \sqrt{2\lambda b}$, which satisfies the lower bounded norm condition in Assumption 4.

• **Well-Specification:** Again, Assumption 1 states that for fixed context u , we have $\mathbb{E}[Y | u] = x^*(\theta^*; u) \in \mathcal{X}(u)$. This suggests

$$\max_{x \in \mathcal{X}(u)} h(\theta^*; u)^\top x = h(\theta^*; u)^\top \mathbb{E}[Y | u]. \quad (\text{EC.3.1})$$

For any fixed context u , there exists a parameter $\theta_\lambda \in \Theta$ such that

$$h(\theta_\lambda; u) = h(\theta^*; u) + \lambda \mathbb{E}[Y | u].$$

Let $\Omega(x) = \frac{1}{2} \|x\|_2^2$ be the square l_2 -norm regularization function, we then have

$$\max_{x \in \mathcal{X}(u)} \{h(\theta_\lambda; u)^\top x - \lambda \Omega(x)\} = \max_{x \in \mathcal{X}(u)} \{h(\theta^*; u)^\top x + \lambda \mathbb{E}[Y | u]^\top x - \frac{\lambda}{2} \|x\|_2^2\}. \quad (\text{EC.3.2})$$

According to Equation (EC.3.1), the first term in Equation (EC.3.2), $h(\theta^*; u)^\top x$, is maximized at $x = \mathbb{E}[Y | u]$ over the feasible region $\mathcal{X}(u)$. The rest of the terms $\lambda \mathbb{E}[Y | u]^\top x - \frac{\lambda}{2} \|x\|_2^2$ are concave in x , which is also maximized at $x = \mathbb{E}[Y | u]$. Therefore, we have

$$\mathbb{E}[Y | u] = \arg \max_{x \in \mathcal{X}(u)} \{h(\theta_\lambda; u)^\top x - \lambda \Omega(x)\},$$

which leads to the result $x_\lambda^*(\theta_\lambda; u) = \mathbb{E}[Y | u]$. Therefore, the parameter space Θ_λ satisfies the well-specification condition in Assumption 4.

EC.3.1. Supplementary for Section 4.1

In this section, we analyze the upper bound for the expected decision error by providing the following modified calibration bound for $D(\hat{\theta}_\lambda, \theta)$ under Assumption 4. The key difference is that, the excess FY risk $R_\lambda(\theta) - \inf_{\theta \in \Theta} R_\lambda(\theta)$ is now evaluated on the space Θ instead of the \mathbb{R}^d space.

THEOREM EC.2 (Restricted Calibration Bound). *Suppose Assumptions 1, 2 and 4 hold. The function Ω is 1-strongly convex. For any $\lambda > 0$ and $\theta \in \mathbb{R}^p$, we have*

$$D(\theta, \theta^*) = R(\theta) - R(\theta^*) \leq \underbrace{2 \mathbb{E}[\|x_\lambda^*(\theta; U) - x^*(\theta; U)\|_2^2]}_{\text{Regularization Error}} + \frac{4}{\lambda} \underbrace{[R_\lambda(\theta) - \inf_{\theta \in \Theta} R_\lambda(\theta)]}_{\text{Excess FY Risk}}.$$

As we argue in Section EC.2.2, the expected decision error $D(\theta, \theta^*)$ can be upper bounded by

$$D(\theta, \theta^*) = \mathbb{E}[\|x^*(\theta; U) - x^*(\theta^*; U)\|_2^2] \leq 2\mathbb{E}\|x^*(\theta; U) - x_\lambda^*(\theta; U)\|_2^2 + 2\mathbb{E}\|x_\lambda^*(\theta; U) - x^*(\theta^*; U)\|_2^2.$$

Therefore, we aim to establish the bound for $\|x_\lambda^*(\theta; U) - x^*(\theta^*; U)\|_2^2$ in terms of the excess FY risk evaluated on the restricted parameter space Θ , i.e., $R(\theta) - \inf_{\theta \in \Theta} R(\theta)$.

PROPOSITION EC.1. *Suppose Assumption 1 holds. Let Θ be a parameter space such that Assumption 4 holds. We have, for any parameter θ ,*

$$\|x_\lambda^*(\theta; u) - x^*(\theta^*; u)\|_2^2 \leq \frac{2}{\lambda} [R_\lambda(\theta; u) - \inf_{\theta \in \Theta} R_\lambda(\theta; u)].$$

Proof of Proposition EC.1 By Assumption 4, we have for every fixed context u , there exists a parameter $\theta_\lambda \in \Theta$ such that

$$x_\lambda^*(\theta_\lambda; u) = \mathbb{E}[Y | u].$$

According to the zero-loss properties of Fenchel-Young loss in Proposition 2, we have

$$L_\lambda(\theta_\lambda; u, \mathbb{E}[Y | u]) = 0.$$

Along with Equations (EC.2.3) and (EC.2.4), this result indicates that the conditional FY risk is minimized at θ_λ for every fixed context u :

$$\begin{aligned} R_\lambda(\theta_\lambda; u) &= L_\lambda(\theta_\lambda; u, \mathbb{E}[Y | u]) + \lambda(\mathbb{E}[\Omega(Y) | u] - \Omega(\mathbb{E}[Y | u])) \\ &= 0 + \lambda(\mathbb{E}[\Omega(Y) | u] - \Omega(\mathbb{E}[Y | u])) = \inf_{\theta} R_\lambda(\theta; u). \end{aligned}$$

Therefore, for any parameter θ , we have

$$R_\lambda(\theta; u) - \inf_{\theta \in \Theta} R_\lambda(\theta; u) = R_\lambda(\theta; u) - R_\lambda(\theta_\lambda; u) = R_\lambda(\theta; u) - \inf_{\theta} R_\lambda(\theta; u). \quad (\text{EC.3.3})$$

By Equations (EC.2.8) and (EC.3.3), we have for any fixed context u and parameter θ ,

$$\frac{\lambda}{2} \|x^*(\theta^*; u) - x_\lambda^*(\theta; u)\|_2^2 \leq R_\lambda(\theta; u) - \inf_{\theta \in \Theta} R_\lambda(\theta; u).$$

Taking the expectation over context U on both sides, we have

$$\begin{aligned} \mathbb{E} \|x_\lambda^*(\hat{\theta}_\lambda; U) - x_\lambda^*(\theta_\lambda^*; U)\|_2^2 &\leq \frac{2}{\lambda} \mathbb{E} \left[R_\lambda(\hat{\theta}_\lambda; U) - \inf_{\theta \in \Theta} R_\lambda(\theta; U) \right] = \frac{2}{\lambda} \left[R_\lambda(\hat{\theta}_\lambda) - \mathbb{E} \left[\inf_{\theta \in \Theta} R_\lambda(\theta; U) \right] \right] \\ &= \frac{2}{\lambda} \left[R_\lambda(\hat{\theta}_\lambda) - \inf_{\theta \in \Theta} \mathbb{E} [R_\lambda(\theta; U)] \right] = \frac{2}{\lambda} \left[R_\lambda(\hat{\theta}_\lambda) - \inf_{\theta \in \Theta} R_\lambda(\theta) \right]. \end{aligned}$$

The interchange of expectation and infimum over Θ in the last line is justified by the fact that the parameter space Θ is compact and the conditional FY risk $R_\lambda(\theta; u) = \mathbb{E}[L_\lambda(\theta; u, Y) | U = u]$ is continuous in θ for any given context u (according to the continuity of Fenchel-Young loss in Proposition 2).

EC.3.1.1. Regularization Error

Lipschitzness of Regularized Oracle under Ball Constraint In this part, we prove the Lipschitzness of optimal regularized solution $x_\lambda^*(\theta; u)$ with respect to λ under the ball constraint and the squared l_2 -norm regularization for any parameter $\theta \in \mathbb{R}^p$ under the fixed context u . The Lipschitzness of regularized oracle is essential for establishing the generalization error bound of the regularized hypothesis.

Fix the context $u \in \mathbb{R}^m$ and parameter $\theta \in \mathbb{R}^p$. Consider the FOP in Equation (1) with l_2 ball constraints and assume the radius of ball is $r(u) = 1$. Given any parameter $\theta \in \mathbb{R}^p$, the optimal unregularized solution is defined as

$$x^*(\theta; u) := \max\{h(\theta; u)^\top x \mid \|x\|_2 \leq 1, x \in \mathbb{R}^d\} = \frac{h(\theta; u)}{\|h(\theta; u)\|_2} \quad (\text{EC.3.4})$$

and the optimal λ -regularized solution is

$$x_\lambda^*(\theta; u) := \max_x \{h(\theta; u)^\top x - \lambda/2\|x\|_2^2 \mid \|x\|_2 \leq 1, x \in \mathbb{R}^d\} = \min \left\{ \frac{h(\theta; u)}{\|h(\theta; u)\|_2}, \frac{h(\theta; u)}{\lambda} \right\}. \quad (\text{EC.3.5})$$

As a result, there is a critic value $\lambda_c(\theta; u) = \|h(\theta; u)\|_2$ such that when $0 \leq \lambda \leq \lambda_c(\theta; u)$, we have $x_\lambda^*(\theta; u) = \frac{h(\theta; u)}{\lambda}$, leading to the regularization error $\|x_\lambda^*(\theta; u) - x^*(\theta; u)\|_2 = 0$. When $\lambda > \lambda_c(\theta; u)$, the optimal regularized solution is $x_\lambda^*(\theta; u) = h(\theta; u)/\lambda$. The next theorem provides the bound of the regularization error $\|x_\lambda^*(\theta; u) - x^*(\theta; u)\|_2$ for any given parameter θ and context u .

THEOREM EC.3 (Lipschitzness of Regularized Solution under Ball Constraint). *Fix context $u \in \mathbb{R}^m$ and parameter $\theta \in \mathbb{R}^p$. Suppose the feasible set $\mathcal{X}(u) := \{x \in \mathbb{R}^d \mid \|x\|_2 \leq a(u)\}$ is a ball constraint with radius $a(u) > 0$, and the regularization function is $\Omega(x) = 1/2\|x\|_2^2$. If the critic value $\lambda_c(\theta; u) := \|h(\theta; u)\|/a(u)$ is positive, we then have*

$$\begin{cases} \|x_\lambda^*(\theta; u) - x^*(\theta; u)\|_2 = 0, & 0 \leq \lambda \leq \lambda_c(\theta; u), \\ \|x_\lambda^*(\theta; u) - x^*(\theta; u)\|_2 \leq \lambda \frac{a(u)^2}{2\|h(\theta; u)\|_2}, & \lambda > \lambda_c(\theta; u). \end{cases}$$

Proof of Theorems 3 and EC.3 Without loss of generality, we assume that the radius of the ball constraint is $a(u) = 1$, and the critic value is then $\lambda_c(\theta; u) = \|h(\theta; u)\|_2$.

According to Equations (EC.3.4) and (EC.3.5), when $0 \leq \lambda \leq \lambda_c(\theta; u)$, we have zero regularization error:

$$\|x_\lambda^*(\theta; u) - x^*(\theta; u)\|_2 = \|x^*(\theta; u) - x^*(\theta; u)\|_2 = 0.$$

When $\lambda > \lambda_c(\theta; u)$, the optimal solution of regularized model is $x_\lambda^*(\theta; u) = h(\theta; u)/\lambda \in \mathcal{X}(u)$, which lies in the interior of feasible set $\mathcal{X}(u)$ and aligns with cost vector $h(\theta; u)$ and unregularized optimal solution $x^*(\theta; u)$. Therefore, we have

$$\|x_\lambda^*(\theta; u) - x^*(\theta; u)\|_2 = \frac{h(\theta; u)^\top (x^*(\theta; u) - x_\lambda^*(\theta; u))}{\|h(\theta; u)\|_2}.$$

By the definition of optimal regularized solution in Equation (12), we have

$$h(\theta; u)^\top x_\lambda^*(\theta; u) - \lambda/2\|x_\lambda^*(\theta; u)\|_2^2 \geq h(\theta; u)^\top x^*(\theta; u) - \lambda/2\|x^*(\theta; u)\|_2^2,$$

which suggests that

$$h(\theta; u)^\top [x^*(\theta; u) - x_\lambda^*(\theta; u)] \leq \lambda/2[\|x^*(\theta; u)\|_2^2 - \|x_\lambda^*(\theta; u)\|_2^2] \leq \lambda/2 \sup_{x \in \mathcal{X}(u)} \|x\|_2^2.$$

Combining the results above, we have for $\lambda > \lambda_c$,

$$\|x_\lambda^*(\theta; u) - x^*(\theta; u)\|_2 \leq \lambda \frac{\sup_{x \in \mathcal{X}(u)} \|x\|_2^2}{2\|h(\theta; u)\|_2} = \lambda \frac{1}{2\|h(\theta; u)\|_2}.$$

EC.3.1.2. Bound for Excess FY Risk To provide the generalization error bound for the excess FY risk $R_\lambda(\theta) - \inf_{\theta \in \Theta} R_\lambda(\theta)$, we introduce the empirical Rademacher complexity $\widehat{\mathcal{R}}_\lambda(\Theta)$ over Θ .

$$\widehat{\mathcal{R}}_\lambda(\Theta) := \mathbb{E}_\sigma \left[\sup_{\theta \in \Theta} \frac{1}{n} \sum_{i=1}^n \sigma_i \tilde{L}_\lambda(\theta; U_i, Y_i) \right].$$

where $\tilde{L}(\theta; U_i, Y_i) := L_\lambda(\theta; U_i, Y_i) - \mathbb{E}_p[L_\lambda(\theta; U_i, Y_i)]$ is a centered Fenchel-Young loss, and $\sigma = \{\sigma_1, \dots, \sigma_n\}$ is a Rademacher sequence. We then have the following generalization bound for the excess FY risk.

LEMMA EC.2 (Symmetrization Bound, Wainwright (2019) - Theorem 4.10). *Suppose the parameter space Θ is bounded. For every finite context u and decision y , the FY loss $L_\lambda(\theta; u, y)$ is also uniformly bounded over Θ by some constant, say c . For any fixed $\lambda > 0$, we have, with probability at least $1 - \delta$,*

$$R_\lambda(\hat{\theta}_\lambda) - \inf_{\theta} R_\lambda(\theta) \leq 2\widehat{\mathcal{R}}_\lambda(\Theta) + \sqrt{\frac{2c^2 \log(1/\delta)}{n}}.$$

REMARK EC.1 (RADEMACHER COMPLEXITY AND VC DIMENSION OF FENCHEL-YOUNG LOSS). The empirical Rademacher complexity, $\widehat{\mathcal{R}}_\lambda(\Theta)$, quantifies the complexity of the parameter space Θ in relation to the Fenchel-Young loss $L_\lambda(\theta; u, y)$. This complexity is closely tied to the VC dimension of the Fenchel-Young loss, which reflects the capacity of the hypothesis space Θ to fit training data. While Assumption 3 assumes that the cost function $h(\theta; u)$ is linear in $\theta \in \mathbb{R}^d$, the Fenchel-Young loss $L_\lambda(\theta; u)$ incorporates the maximization of $h(\theta; u)^\top x$ over the convex feasible region $\mathcal{X}(u)$. This introduces piecewise linearity in $L_\lambda(\theta; u)$, with the structure of its pieces determined by the specific form of $\mathcal{X}(u)$. Consequently, the VC dimension of the Fenchel-Young loss is typically greater than that of the cost function $h(\theta; u)$.

REMARK EC.2 (VC DIMENSION OF FENCHEL-YOUNG LOSS FOR BALL CONSTRAINED FOP).

For fixed context u , if the FOP in Equation (1) is bilinear in both decision x and parameter θ , equipped with ball constraint $\mathcal{X}(u) = \{x \in \mathbb{R}^d \mid \|x\|_2 \leq a(u)\}$, we can establish the finite-sample bound for empirical Rademacher complexity $\widehat{\mathcal{R}}_\lambda(\Theta)$, and therefore the estimation error $\|x_\lambda^*(\hat{\theta}_\lambda; u) - x_\lambda^*(\theta_\lambda^*; u)\|_2$ through calibration bound in Theorem 1 and Lemma 2. Without loss of generality, we assume the radius of the ball constraint is $a(u) = 1$ for every context u and the critic value $\lambda_c(\theta; u) = \|h(\theta; u)\|_2$ is positive. As a consequence, for fixed parameter θ context u and $\lambda < \lambda_c(\theta; u)$, the solution of $\max_{x \in \mathcal{X}(u)} \{h(\theta; u)^\top x - \lambda/2 \|x\|_2^2\}$ is $x_\lambda^*(\theta; u) = h(\theta; u) / \|h(\theta; u)\|_2$. The corresponding Fenchel-Young loss can then be written as

$$\begin{aligned} L_\lambda(\theta; u, y) &= \max_{x \in \mathcal{X}(u)} \{h(\theta; u)^\top x - \lambda/2 \|x\|_2^2\} - \{h(\theta; u)^\top y - \lambda/2 \|y\|_2^2\} \\ &= \|h(\theta; u)\|_2 - \lambda/2 - h(\theta; u)^\top y + \lambda/2 \|y\|_2^2 \\ &= \|h(\theta; u)\|_2 - h(\theta; u)^\top y + \lambda/2 (\|y\|_2^2 - 1). \end{aligned}$$

By Assumption 3, the cost function $h(\theta; u)$ is linear in θ , and the Fenchel-Young loss $L_\lambda(\theta; u, y)$ is then linear in θ for fixed context u and decision y . The Rademacher complexity of the parameter space Θ with respect to the Fenchel-Young loss $L_\lambda(\theta; u, y)$ is then the same as the Rademacher complexity of the parameter space $\Theta \subseteq \mathbb{R}^d$ with respect to the cost function $h(\theta; u)$, which is at most $(d+1)$.

EC.3.2. Supplementary for Section 4.2

We now establish the theoretical guarantees for the decision regret $\text{Reg}(\hat{\theta}_\lambda, \theta^*)$ and the parameter error $E(\hat{\theta}_\lambda, \theta^*)$ defined in Equations (5) and (6) respectively.

Decision Regret With the Cauchy-Schwarz inequality, we establish the following bound for the decision regret $\text{Reg}(\hat{\theta}_\lambda, \theta^*)$ in terms of the decision error $D(\hat{\theta}_\lambda, \theta^*)$. Formally, Theorem 4 states that if the expected squared norm of the true cost function $h(\theta^*; U)$ is bounded by some constant, say $\mathbb{E}[\|h(\theta^*; U)\|_2^2] \leq B$, we have

$$\text{Reg}(\hat{\theta}_\lambda, \theta^*) \leq BD(\hat{\theta}_\lambda, \theta^*).$$

Proof of Theorem 4 According to the definition of decision regret in Equation (5), we have

$$\begin{aligned} \text{Reg}(\hat{\theta}_\lambda, \theta^*) &= \mathbb{E} \left[h(\theta^*; U)^\top (x^*(\hat{\theta}_\lambda; U) - x^*(\theta^*; U)) \right] \\ &\leq \mathbb{E} \left[\|h(\theta^*; U)\|_2 \cdot \|x^*(\hat{\theta}_\lambda; U) - x^*(\theta^*; U)\|_2 \right] \\ &\leq \mathbb{E}[\|h(\theta^*; U)\|_2^2] \cdot \mathbb{E}[\|x^*(\hat{\theta}_\lambda; U) - x^*(\theta^*; U)\|_2^2] \\ &\leq BD(\hat{\theta}_\lambda, \theta^*). \end{aligned}$$

The first and second inequality follow from the Cauchy-Schwarz inequality. The third inequality is due to the boundedness of the expected squared norm of the true cost function $h(\theta^*; U)$.

Parameter Error By assuming the identifiability condition proposed in Aswani et al. (2018, IC Conditions), we analyze the convergence of parameter error $E(\hat{\theta}_\lambda, \theta^*)$ in terms of the convergence of decision error $D(\hat{\theta}_\lambda, \theta^*)$.

THEOREM EC.4 (Uniform Convergence of Parameter Error). *Suppose Assumption 2 holds, and for all $\theta \in \Theta \setminus \theta^*$, $\text{dist}(\mathcal{X}^*(\theta; u), \mathcal{X}^*(\theta^*; u)) > 0$. Then for any θ such that $x^*(\theta; u) \rightarrow_p x^*(\theta^*; u)$, we have $\theta \rightarrow_p \theta^*$.*

Theorem 5 establishes the statistical convergence of decision error $D(\hat{\theta}_\lambda, \theta^*)$ implies the statistical convergence of parameter error $E(\hat{\theta}_\lambda, \theta^*)$ to zero.

Proof of Theorem 5 For fixed context u , since the feasible region $\mathcal{X}(u)$ does not rely on θ in our setting, $\mathcal{X}(u)$ is continuous in $\theta \in \Theta$. Therefore, we can apply Berge Maximum Theorem (Berge 1877) and claims that the optimal solution set $\mathcal{X}^*(\theta; u)$ is upper hemicontinuous in θ . Moreover, as $\mathcal{X}^*(\theta; u)$ is almost surely singleton and $\text{dist}(\mathcal{X}^*(\theta; u), \mathcal{X}^*(\theta^*; u)) > 0$ for every context u , by applying Theorem 5.14 of Van der Vaart (2000), we have $\theta \rightarrow_p \theta^*$ if $x^*(\theta; u) \rightarrow x^*(\theta^*; u)$.

EC.4. Additional Experimental Details

In Section 5, we provide synthetic data experimental results and real data experimental results for different methods. In this section, we further explain the details of these experiments setup, implementation, and provide additional experimental results. All experiments are implemented on a cloud computing platform with 128 CPUs of model Intel(R) Xeon(R) Platinum 8369B CPU @ 2.70GHz, 250GB RAM and 500GB storage.

EC.4.1. Synthetic Data Experiment Setups and Implementation details

We present several numerical results, including both linear and nonlinear examples, that demonstrate the great advantages in time consuming, parameter estimation accuracy, optimal solution gap and objective function value gap. Specifically, we study three inverse optimization scenarios for each example.

- **Noisy Decision:** The observed solution is equal to the real optimal solution plus a noise drawing from the standard normal distribution. For example, if true optimization solution for the forward optimization problem(FOP) is $x^* \in \mathbb{R}^p$, then the observed solution is $y = x^* + w$, where every element of $w \in \mathbb{R}^p$ draws from a standard normal distribution. It is worth noting that the observed solution in this case may not even be feasible, so many classical inverse optimization methods do not handle this situation well.

- **Noisy Objective Function:** The observed solution is the optimal solution corresponding to the key term $\theta + u$ of the objective function plus the standard normal distribution noise. For example, if the true forward optimization problem(FOP) is $\min\{(\theta + u)^\top x \mid x \in [0, 1]^p\}$, then the observed solution corresponds to the optimal solution of the optimization problem $\min\{(\theta + u + w)^\top x \mid x \in [0, 1]^p\}$, where every element of $w \in \mathbb{R}^p$ drawn from a standard normal distribution.

- **Noiseless:** The observed solution is the optimal solution to the true forward optimization problem without any noise.

We repeated this 100 times for each example and uniformly used a random number seed with the same number to ensure fairness. We implement various methods with sample sizes of 50, 100, 300, 500, and 1000, utilizing the Gurobi solver for all experiments. The following metrics are collected:

- **Time:** The total time required to complete 100 serial repetitions of the experiment using the specified method.

- **Parameter Error:** The l_1 norm of the difference between the estimated parameter $\hat{\theta}$ and the true parameter θ^* , denoted as $E(\hat{\theta}, \theta^*) := \|\hat{\theta} - \theta^*\|_1$ in Equation (6).

- **Decision Error:** The squared l_2 norm of the difference between the optimal solution $x^*(\hat{\theta}; u)$ based on the estimated $\hat{\theta}$ and the optimal solution $x^*(\theta^*; u)$ based on the true parameter θ^* given context u , denoted $D(\hat{\theta}, \theta^*; u) := \|x^*(\hat{\theta}; u) - x^*(\theta^*; u)\|_2^2$ as shown in Section 4.1.

• **Regret:** The gap between the objective function value of the actual decision and the true optimal objective function value. For example, given context u , if the forward optimization problem is $\min\{h(\theta^*; u)^\top x \mid g(u, x) \preceq 0\} = \max\{-h(\theta^*; u)^\top x \mid g(u, x) \preceq 0\}$ with the corresponding optimization solution $x^*(\theta^*; u)$ the conditional decision regret is then $\text{Reg}(\hat{\theta}, \theta^*; u) := h(\theta^*; u)^\top x^*(\hat{\theta}; u) - h(\theta^*; u)^\top x^*(\theta^*; u)$ as shown in Equation (5).

To fully illustrate the effectiveness and advantages of our method, in each set of experiments, we compared the Fenchel-Young loss method with a number of classical inverse optimization methods, which are SPA Aswani et al. (2018), approximate KKT conditions(KKA) Keshavarz et al. (2011), variational inequality approximate(VIA) Bertsimas et al. (2015), and maximum optimality margin(MOM) Sun et al. (2023). Among these, the maximum optimality margin (MOM) method models the basic and non-basic variables in the observed solution when the forward optimization problem (FOP) is a linear programming problem. However, in the Noisy Decision setting, the observed optimal solution is not at the vertex of the feasible set. Therefore, this method is not suitable for the Noisy Decision setting, nor is it suitable when the FOP is a nonlinear programming problem.

We design five different synthetic data experiments. The first three experiments involve linear programming forward optimization problems, which include box constraints and half-space constraints. The objective functions are of the form $\theta + u$ and $\theta \circ u$, where θ is the unknown parameter vector to be estimated, and u is the known context vector. The last two experiments involve forward optimization problems of nonlinear programming: the first is quadratic in x with a box constraint, and the second is linear in X with a feasible set defined by a ball constraint.

We will show that our method is the best, or close to the best, in Noisy Decision setting, Noisy Objective Function setting, or Noiseless setting. Compared with other classical inverse optimization methods, in all kinds of forward optimization problem(FOP), it has significant advantages in parameter recovery, decision making and computational time.

EC.4.1.1. Example A In this experiment, we consider optimization problems with more complex constraints,

$$\min\{(\theta + u)^\top x \mid x \succeq 0, \|x\|_1 \leq a\} = \min\left\{\sum_{k=1}^p (\theta_k + u_k)x_k \mid x \succeq 0, \|x\|_1 \leq a\right\}.$$

Every element of context vector $u \in \mathbb{R}^p$ has a uniform distribution with support $[-1, 1]^p$ and $p = 10$. In addition, we set $a = 3$ and true parameter vector $\theta = [0.5, \dots, 0.5] \in \mathbb{R}^p$. The optimal solution x^{opt} to this problem is

$$x^*(\theta; u)_k = \begin{cases} a, & \text{if } (\theta_k + u_k) \leq 0 \\ 0, & \text{otherwise.} \end{cases}$$

To compute the Fenchel-Young loss, we first derive the convex conjugate of Ω , which is

$$\max_{x \in \mathcal{X}(u)} V_\lambda(\theta; u, x) = \max_{x \in \mathcal{F}} \left\{ -(\theta + u)^\top x - \frac{\lambda}{2} x^\top x \right\} \rightarrow x_\lambda^*(\theta; u).$$

Here $\mathcal{F} : \{x \in \mathbb{R}^p | x \succeq 0, \sum_{i=1}^p x_i \leq a\}$ is the feasible region of this example, and $x_\lambda^*(\theta; u)$ is the regularized optimal solution. Therefore, based on the observation solution y , we have the following expression of Fenchel-Young loss,

$$\begin{aligned} L_\lambda(\theta; u, y) &= \max_{x \in \mathcal{X}(u)} V_\lambda(\theta; u, x) + \lambda \Omega(y) - \left[-\sum_{k=1}^p (\theta_k + u_k) y_k \right] \\ &= \max_{x \in \mathcal{X}(u)} V_\lambda(\theta; u, x) + \lambda \Omega(y) + \sum_{k=1}^p (\theta_k + u_k) y_k \end{aligned}$$

Then, we have the gradient of Fenchel-Young Loss:

$$\nabla_{\theta_k} L_\lambda(\theta; u, y) = [-x_\lambda^*(\theta; u)_k + y_k]$$

for $k = 1, \dots, p$. In this experiment, we cannot directly write the explicit expression for $x^*(\theta, u)$, so we need to deploy the solver every time in the experiment, which may result in a long computational time. However, we can choose to use a stochastic gradient descent algorithm to speed up our method and still ensure that the computational time of our method is acceptable.

Result Discussion The results of experiments in the Noisy Decision setting, the Noisy Objective Function setting, and the Noiseless setting, which are shown in Table EC.1, Table EC.2 and Table EC.3 respectively, average over 100 repetitions. Based on the experimental results, we can draw the following conclusions.

- In the Noisy Decision setting and the Noisy Objective Function setting, our method based on the Fenchel-Young loss demonstrates superior performance in terms of parameter error, decision error, and regret. Specifically, it achieves the lowest values for these metrics compared to other traditional inverse optimization methods. Other methods, except for KKA, show gradual convergence in decision error and regret as the sample size increases. However, their performance in parameter recovery remains consistently poor. In contrast, the KKA method fails to converge in terms of parameter error, decision error, and regret. It seems that KKA always performs well in the noiseless setting and poorly in the noisy setting in the following experiments.

- In the Noiseless setting, the results of our method are very close to those of KKA and VIA, which are considered the best-performing methods. Additionally, it appears that MOM is better suited for decision-making than for parameter recovery. Furthermore, the SPA method performs poorly in terms of parameter error, decision error, and regret. This is because the semi-parametric algorithm in SPA is designed to remove noise. However, in the Noiseless setting, it becomes detrimental to the algorithm's performance.

Table EC.1 The experimental results for various methods under different metrics are presented for the FOP defined as $\min\{(\theta + u)^\top x \mid x \succeq 0, \|x\|_1 \leq a\} = \min\{\sum_{k=1}^p (\theta_k + u_k)x_k \mid x \succeq 0, \|x\|_1 \leq a\}$ in the **Noisy Decision** setting. For the FY loss, we set $\lambda = 0.1$ and $\Omega(x) = 1/2\|x\|_2^2$.

Sample size	Parameter Error				Decision Error				Regret			
	FY	SPA	KKA	VIA	FY	SPA	KKA	VIA	FY	SPA	KKA	VIA
50	1.30	2.46	4.25	3.81	3.03	4.53	7.66	3.90	0.05	0.20	0.77	0.08
100	1.17	1.35	4.58	4.12	2.47	2.94	7.79	3.17	0.03	0.06	0.84	0.05
300	0.53	2.10	4.87	4.42	2.05	2.66	8.22	2.19	0.02	0.08	0.93	0.03
500	0.53	2.44	4.92	4.52	1.64	2.69	8.32	1.88	0.01	0.10	0.95	0.03
1000	0.38	2.59	4.96	4.56	1.33	2.64	8.40	1.60	0.01	0.11	0.96	0.03

Table EC.2 The experimental results for various methods under different metrics are presented for the FOP defined as $\min\{(\theta + u)^\top x \mid x \succeq 0, \|x\|_1 \leq a\} = \min\{\sum_{k=1}^p (\theta_k + u_k)x_k \mid x \succeq 0, \|x\|_1 \leq a\}$ in the **Noisy Objective Function** setting. For the FY loss, we set $\lambda = 0.1$ and $\Omega = 1/2\|x\|_2^2$.

Sample size	Parameter Error					Decision Error					Regret				
	FY	SPA	KKA	VIA	MOM	FY	SPA	KKA	VIA	MOM	FY	SPA	KKA	VIA	MOM
50	1.15	1.84	2.17	2.09	5.91	3.75	5.13	5.50	5.47	6.53	0.04	0.15	0.15	0.11	0.17
100	1.09	0.99	1.93	1.91	5.81	2.81	3.63	4.46	4.00	5.37	0.04	0.05	0.11	0.06	0.11
300	0.37	1.15	2.23	1.84	5.83	2.06	2.32	4.21	2.49	3.55	0.03	0.03	0.14	0.03	0.06
500	0.36	1.43	2.89	1.69	5.81	1.66	2.08	4.70	2.06	3.04	0.01	0.03	0.21	0.02	0.05
1000	0.22	1.48	3.50	1.81	5.82	1.25	1.71	5.46	1.61	2.38	0.00	0.03	0.33	0.02	0.04

Table EC.3 The experimental results for various methods under different metrics are presented for the FOP defined as $\min\{(\theta + u)^\top x \mid x \succeq 0, \|x\|_1 \leq a\} = \min\{\sum_{k=1}^p (\theta_k + u_k)x_k \mid x \succeq 0, \|x\|_1 \leq a\}$ in the **Noiseless** setting. For the FY loss, we set $\lambda = 0.1$ and $\Omega(x) = 1/2\|x\|_2^2$.

Sample size	Parameter Error					Decision Error					Regret				
	FY	SPA	KKA	VIA	MOM	FY	SPA	KKA	VIA	MOM	FY	SPA	KKA	VIA	MOM
50	0.64	2.12	0.96	0.93	5.01	1.05	3.02	0.00	0.00	3.12	0.02	0.10	0.00	0.00	0.06
100	0.70	2.33	0.44	0.42	5.03	1.09	2.89	0.00	0.00	2.76	0.01	0.10	0.00	0.00	0.05
300	0.34	2.67	0.16	0.15	5.07	0.76	2.87	0.00	0.00	2.07	0.00	0.12	0.00	0.00	0.03
500	0.21	2.69	0.08	0.07	5.08	0.63	2.72	0.00	0.00	1.73	0.00	0.12	0.00	0.00	0.03
1000	0.18	2.71	0.04	0.04	5.08	0.53	2.56	0.00	0.00	1.40	0.00	0.12	0.00	0.00	0.03

EC.4.1.2. Example B Next, we consider the following forward optimization problem(FOP),

$$\min\{(\theta \circ u)^\top x \mid x \in [-1, 1]^p\} = \min \left\{ \sum_{k=1}^p (\theta_k \circ u_k) x_k \mid x \in [-1, 1]^p \right\}.$$

Every element of context vector $u \in \mathbb{R}^p$ has a uniform distribution with support $[-1, 1]^p$ and $p = 10$ in our experiments. \circ means Hadamard product, that is, $(\theta \circ u)^\top x = \sum_{i=1}^p \theta_i u_i x_i$. The optimal solution x_{opt} to this problem is

$$x^*(\theta; u)_k = \begin{cases} -1, & \text{if } \theta_k u_k > 0 \\ +1, & \text{if } \theta_k u_k < 0. \end{cases}$$

Note that this problem is not identifiable for the parameter vector $\theta \in \mathbb{R}^p$ that needs to be estimated. Because, as long as we estimate the sign of each component of the parameter vector θ correctly, we can obtain the solution that is exactly consistent with the optimal parameter, which also means the parameter vector θ is not identifiable. Therefore, we set the true parameter vector $\theta = [0.5, -0.5, \dots, -0.5, 0.5, 1] \in \mathbb{R}^p$ to test the sign recognition ability of various inverse optimization methods.

The last element is set to 1 instead of 0.5 because the parameter vector θ solved by the SPA, KKA, and VIA methods will be very close to 0, which may cause the degeneracy. The reasons for this will be explained in the next few paragraphs. Therefore, we need to ensure that the sum of the elements of the real parameter vector θ is not 0, so that we can add constraints such as the sum of the elements of θ is a non-zero constant to prevent the degeneracy of these methods.

To compute the Fenchel-Young loss, we first derive the convex conjugate of Ω , which is

$$\max_{x \in \mathcal{X}(u)} V_\lambda(\theta; u, x) = \max_{x \in [-1, 1]^p} \left\{ -(\theta \circ u)^\top x - \frac{\lambda}{2} x^\top x \right\} \rightarrow x_\lambda^*(\theta; u)_k = \max \left\{ -1, \min \left\{ 1, -\frac{\theta_k u_k}{\lambda} \right\} \right\}.$$

Therefore, based on the observation solution y , we have the following expression of Fenchel-Young loss,

$$\begin{aligned} L_\lambda(\theta; u, y) &= \max_{x \in \mathcal{X}(u)} V_\lambda(\theta; u, x) + \lambda \Omega(y) - \left[-\sum_{k=1}^p (\theta_k \circ u_k) y_k \right] \\ &= \max_{x \in \mathcal{X}(u)} V_\lambda(\theta; u, x) + \lambda \Omega(y) + \sum_{k=1}^p (\theta_k \circ u_k) y_k \end{aligned}$$

Then, we have the gradient of Fenchel-Young Loss: for $k = 1, \dots, p$,

$$\nabla_{\theta_k} L_\lambda(\theta; u, y) = [-u_k x_\lambda^*(\theta; u)_k + u_k y_k] = u_k \left[-\max \left\{ -1, \min \left\{ 1, -\frac{\theta_k u_k}{\lambda} \right\} \right\} + y_k \right].$$

Before showing the experimental results of this example, let us first explain why the KKA, VIA, and SPA methods degenerate. The following is the Lagrangian dual of the forward optimization problem(FOP).

$$\begin{aligned}
L(x, \lambda_1, \lambda_2, u, \theta) &= (\theta \circ u)^\top x + \lambda_1^\top (-1 - x) + \lambda_2^\top (x - 1) \\
&= (\theta \circ u - \lambda_1 + \lambda_2)^\top x - \sum_{k=1}^p (\lambda_{1,k} + \lambda_{2,k}) \\
&= \sum_{k=1}^p (\theta \circ u - \lambda_1 + \lambda_2)_k x_k - \sum_{k=1}^p (\lambda_{1,k} + \lambda_{2,k}).
\end{aligned}$$

where λ_1 and λ_2 are Lagrangian multipliers. By minimizing the x , we obtain the Lagrangian dual function as

$$h(\lambda_1, \lambda_2, u, \theta) = \inf_x L(x, \lambda_1, \lambda_2, u, \theta) = \begin{cases} -\sum_{k=1}^p (\lambda_{1,k} + \lambda_{2,k}), & (\theta \circ u - \lambda_1 + \lambda_2)_k = 0, \forall k \in [p] \\ -\infty, & \text{otherwise.} \end{cases}$$

SPA Method Formulation Therefore, for the SPA method, we are dealing with the following constrained risk minimization problem:

$$\begin{aligned}
\hat{\theta}_n &= \arg \min_{\theta, \lambda_{i,1}, \lambda_{i,2}, \epsilon_i} \frac{1}{n} \sum_{i=1}^n \epsilon_i \\
\text{s.t. } & \sum_{k=1}^p (\theta u_i)_k \bar{y}_{i,k} - \left[-\sum_{k=1}^p (\lambda_{i,1} + \lambda_{i,2})_k \right] \leq \epsilon_i, \quad \forall i \in [n] \\
& (\theta \circ u_i - \lambda_{i,1} + \lambda_{i,2})_k = 0, \quad \forall k \in [p], \forall i \in [n] \\
& \lambda_{i,1} \succeq 0, \quad \forall i \in [n] \\
& \lambda_{i,2} \succeq 0, \quad \forall i \in [n]
\end{aligned}$$

where $\bar{y}_{i,k}$ is the value of the k -th element of the i -th data observation solution vector after noise removal by the semi-parametric algorithm.

VIA Method Formulation For the VIA method, given a sequence of observation y_j for $j = 1, \dots, N$, we have the following optimization problem:

$$\begin{aligned}
\min_{\theta, \lambda_{1,i}, \lambda_{2,i}, \epsilon_i} & \|\epsilon\|_2^2 \\
\text{s.t. } & (\theta \circ u_i)^\top y_i - \left[-\sum_{k=1}^p (\lambda_{1,i,k} + \lambda_{2,i,k}) \right] \leq \epsilon_i, \quad \forall i \in [n] \\
& (\theta \circ u_i - \lambda_{1,i} + \lambda_{2,i})_k = 0, \quad \forall k \in [p], \forall i \in [n] \\
& \lambda_{1,j} \succeq 0, \lambda_{2,j} \succeq 0 \quad \forall i \in [n]
\end{aligned}$$

KKA Method Formulation For the KKA method, we need to solve the following optimization problem.

$$\begin{aligned}
& \min_{\theta, \lambda_{1,i}, \lambda_{2,i}} \sum_{i=1}^n (\|r_i^{\text{stat}}\|_2^2 + \|r_{1,i}^{\text{comp}}\|_2^2 + \|r_{2,i}^{\text{comp}}\|_2^2) \\
& \text{s.t. } r_{i,k}^{\text{stat}}(\theta, \lambda_i, \nu_i) = \theta_k u_{i,k} + \lambda_{1,i} - \lambda_{2,i}, \quad \forall k \in [p], \forall i \in [n] \\
& \quad r_{1,i,k}^{\text{comp}}(\lambda_i) = \lambda_{1,i,k}(x_{i,k} - 1), \quad \forall k \in [p], \forall i \in [n] \\
& \quad r_{2,i,k}^{\text{comp}}(\lambda_i) = \lambda_{2,i,k}(-1 - x_{i,k}), \quad \forall k \in [p], \forall i \in [n] \\
& \quad \lambda_i \succeq 0, \quad \forall i \in [n] \\
& \quad \theta \in [0, 1]^p.
\end{aligned}$$

Based on the above optimization problems, we can find that when θ is equal to a vector with all zeros, the objective function of these three optimization problems can be taken to 0, that is, the minimum value. As a result, this can mislead the solver into solving meaningless solutions such as all zeros, leading to degeneracy of the problem.

Result Discussion The results of experiments in the Noisy Decision setting, the Noisy Objective Function setting, and the Noiseless setting, which are shown in Table EC.4, Table EC.5 and Table EC.6 respectively, average over 100 repetitions. Since the parameter vector θ is not identifiable in this problem, we only need to focus on the decision error and the regret. Thus, we can clearly come to the following conclusion.

- In the Noisy Decision setting and Noisy Objective Function setting, the Fenchel-Young loss and VIA methods exhibit the best performance, achieving zero decision error and regret even with small sample sizes. In contrast, the MOM method requires a larger sample size to reduce these metrics to zero. The KKA and SPA methods perform the worst, with almost no convergence observed.

Furthermore, we observe that the parameter θ estimated by the SPA, KKA, and VIA methods consistently approaches zero, leading to the problem degeneracy. The reason for the degeneracy, as previously explained, is that $\theta = \mathbf{0}$ happens to minimize the optimization objectives of SPA, KKA, and VIA. However, such a θ is meaningless for decision-making. Among these methods, VIA is still able to correctly recover the sign of each element of the vector θ , which helps to maintain good performance in terms of decision error and regret.

To address this issue, we attempted to introduce regularization constraints to these methods. For example, we imposed constraints such as requiring the sum of the elements of the estimated parameter vector θ to be 0.5, or fixing the first element of the parameter vector θ at 0.5. However, these modifications did not significantly improve the experimental results of these methods. In contrast, our proposed method based on the Fenchel-Young loss does not face the challenge of degeneracy and maintains robust performance without the need for such regularization constraints.

Notably, MOM also successfully avoids degeneration, which is in agreement with the conclusions reached by Sun et al. (2023).

- In the Noiseless setting, all methods except SPA achieve very good results, with decision error and regret reaching zero even when the sample size is as small as 50. However, SPA incorporates a semi-parametric algorithm designed to remove noise, which becomes counterproductive in a noiseless environment. If the semi-parametric algorithm is removed, the method essentially becomes equivalent to VIA. Additionally, compared to the noisy settings, KKA is able to obtain a correctly signed parameter vector instead of a degenerate all-zero vector in this noiseless setting.

Table EC.4 The experimental results for various methods under different metrics are presented for the FOP defined as $\min\{(\theta \circ u)^\top x \mid x \in [-1, 1]^p\} = \min\{\sum_{k=1}^p (\theta_k * u_k)x_k \mid x \in [-1, 1]^p\}$ in the **Noisy Decision** setting. For the FY loss, we set $\lambda = 0.1$ and $\Omega(x) = 1/2\|x\|_2^2$.

Sample size	Parameter Error				Decision Error				Regret			
	FY	SPA	KKA	VIA	FY	SPA	KKA	VIA	FY	SPA	KKA	VIA
50	2.76	5.50	5.50	5.50	0.00	19.99	19.99	0.00	0.00	2.75	2.75	0.00
100	2.42	5.50	5.50	5.50	0.00	19.99	19.99	0.00	0.00	2.76	2.76	0.00
300	2.25	5.50	5.50	5.50	0.00	20.00	20.00	0.00	0.00	2.75	2.75	0.00
500	2.27	5.50	5.50	5.50	0.00	20.01	20.01	0.00	0.00	2.76	2.76	0.00
1000	2.19	5.50	5.50	5.50	0.00	19.99	19.99	0.00	0.00	2.75	2.75	0.00

Table EC.5 The experimental results for various methods under different metrics are presented for the FOP defined as $\min\{(\theta \circ u)^\top x \mid x \in [-1, 1]^p\} = \min\{\sum_{k=1}^p (\theta_k * u_k)x_k \mid x \in [-1, 1]^p\}$ in the **Noisy Objective Function** setting. For the FY loss, we set $\lambda = 0.1$ and $\Omega = 1/2\|x\|_2^2$.

Sample size	Parameter Error					Decision Error					Regret				
	FY	SPA	KKA	VIA	MOM	FY	SPA	KKA	VIA	MOM	FY	SPA	KKA	VIA	MOM
50	2.78	5.50	5.50	5.50	7.94	0.00	19.99	19.99	2.04	1.96	0.00	2.75	2.75	0.25	0.24
100	2.80	5.50	5.50	5.50	7.27	0.00	19.99	19.99	0.20	0.16	0.00	2.76	2.76	0.03	0.02
300	2.80	5.50	5.50	5.50	7.22	0.00	20.00	20.00	0.00	0.00	0.00	2.75	2.75	0.00	0.00
500	2.80	5.50	5.50	5.50	7.22	0.00	20.01	20.01	0.00	0.00	0.00	2.76	2.76	0.00	0.00
1000	2.80	5.50	5.50	5.50	7.17	0.00	19.99	19.99	0.00	0.00	0.00	2.75	2.75	0.00	0.00

Table EC.6 The experimental results for various methods under different metrics are presented for the FOP defined as $\min\{(\theta \circ u)^\top x \mid x \in [-1, 1]^p\} = \min\{\sum_{k=1}^p (\theta_k * u_k)x_k \mid x \in [-1, 1]^p\}$ in the **Noiseless** setting. For the FY loss, we set $\lambda = 0.1$ and $\Omega(x) = 1/2\|x\|_2^2$.

Sample size	Parameter Error					Decision Error					Regret				
	FY	SPA	KKA	VIA	MOM	FY	SPA	KKA	VIA	MOM	FY	SPA	KKA	VIA	MOM
50	2.22	5.50	4.50	4.33	31.27	0.00	20.00	0.00	0.00	0.00	0.00	20.00	0.00	0.00	0.00
100	2.22	5.50	4.50	4.39	31.24	0.00	20.00	0.00	0.00	0.00	0.00	20.00	0.00	0.00	0.00
300	2.22	5.50	4.50	4.45	31.26	0.00	20.00	0.00	0.00	0.00	0.00	20.00	0.00	0.00	0.00
500	2.22	5.50	4.50	4.48	31.29	0.00	20.01	0.00	0.00	0.00	0.00	20.01	0.00	0.00	0.00
1000	2.22	5.50	4.50	4.49	31.32	0.00	20.00	0.00	0.00	0.00	0.00	20.00	0.00	0.00	0.00

EC.4.1.3. Example C Next, we consider the following forward optimization problem (FOP),

$$\min\{(\theta + u)^\top x \mid x \in [-1, 1]^p\} = \min\left\{\sum_{k=1}^p (\theta_k + u_k)x_k \mid x \in [-1, 1]^p\right\}.$$

Every element of context vector $u \in \mathbb{R}^p$ has a uniform distribution with support $[-1, 1]^p$ and $p = 10$ in our experiments. Apparently, the optimal solution x^{opt} to this problem is

$$x^*(\theta; u)_k = \begin{cases} -1, & \text{if } \theta_k + u_k > 0 \\ +1, & \text{if } \theta_k + u_k \leq 0. \end{cases}$$

We set the true parameter vector $\theta = [0.5, \dots, 0.5]^p \in \mathbb{R}^p$, which needs to be estimated. In addition, our method uniformly uses the l_2 regular term, which is $\frac{\lambda}{2}\|x\|_2^2$, in all experiments.

To compute the Fenchel-Young loss, we first derive the convex conjugate of Ω , which is

$$\max_{x \in \mathcal{X}(u)} V_\lambda(\theta; u, x) = \max_{x \in [-1, 1]^p} \left\{ -(\theta + u)^\top x - \frac{\lambda}{2} x^\top x \right\} \rightarrow x_\lambda^*(\theta; u)_k = \max \left\{ -1, \min \left\{ 1, -\frac{\theta_k + u_k}{\lambda} \right\} \right\}.$$

Therefore, based on the observation solution y , we have the following expression of Fenchel-Young loss,

$$L_\lambda(\theta; u, y) = \max_{x \in \mathcal{X}(u)} V_\lambda(\theta; u, x) + \lambda \Omega(y) - \left[-\sum_{k=1}^p (\theta_k + u_k)y_k \right] = \max_{x \in \mathcal{X}(u)} V_\lambda(\theta; u, x) + \lambda \Omega(y) + \sum_{k=1}^p (\theta_k + u_k)y_k$$

Then, we have the gradient of Fenchel-Young Loss:

$$\nabla_{\theta_k} L_\lambda(\theta; u, y) = [-x_\lambda^*(\theta; u)_k + y_k] = \left[-\max \left\{ -1, \min \left\{ 1, \frac{\theta_k + u_k}{\lambda} \right\} \right\} + y_k \right]$$

for $k = 1, \dots, p$. Finally, we can utilize the gradient descent algorithm to optimize the parameter vector θ .

Result Discussion The results of experiments in the Noisy Decision setting, the Noisy Objective Function setting, and the Noiseless setting, which are shown in Table EC.7, Table EC.8 and Table EC.9 respectively, average over 100 repetitions. Based on these results, we can draw the following conclusions.

- In the Noisy Decision setting, our method shows significant advantages over other inverse optimization methods in both parameter estimation and decision-making. The parameter error, decision error, and regret are the lowest among all methods and decrease rapidly as the sample size increases. Moreover, the SPA method outperforms the VIA method in terms of parameter error, decision error, and regret. This superior performance may be attributed to the semi-parametric algorithm in SPA, which effectively mitigates the impact of noise.

- In the Noisy Objective Function setting, our method achieves the lowest parameter error, decision error, and regret. Specifically, because standard normal distribution noise w is added to $\theta + u$, the problem becomes more complex. If $\theta + u + w \leq 0$, the observed solution is 1; otherwise, it is -1. This scenario is more challenging than the Noisy Decision setting, where the direct addition of normal distribution noise to the observed solution has a relatively small probability of changing 1 to -1 or -1 to 1. In contrast, in the Noisy Objective Function setting, since u is uniformly distributed from $[-1, 1]^p$ and $\theta = [0.5, \dots, 0.5]^p$, the addition of standard normal distribution noise w is more likely to alter the original sign of $\theta + u$. Consequently, the noise has a more pronounced impact in the Noisy Objective Function setting.

Due to these complexities, all methods perform significantly worse in this setting compared to the Noisy Decision setting, and even the KKA method fails to converge. However, our method remains the best performing approach in this challenging scenario.

- In the Noiseless setting, almost all methods perform well except MOM, particularly in terms of regret, which is expected given its status as a classic setting. However, even with a small sample size, such as 50, our method achieves superior results compared to other classical inverse optimization methods. The inclusion of a semi-parametric algorithm in SPA, designed to remove noise, is redundant in the Noiseless setting and can detract from its performance. In this specific example, removing the semi-parametric algorithm from SPA essentially renders it equivalent to VIA.

Table EC.7 The experimental results for various methods under different metrics are presented for the FOP defined as $\min\{(\theta + u)^\top x \mid x \in [-1, 1]^p\} = \min\{\sum_{k=1}^p (\theta_k + u_k)x_k \mid x \in [-1, 1]^p\}$ in the **Noisy Decision** setting. For the FY loss, we set $\lambda = 0.1$ and $\Omega(x) = 1/2\|x\|_2^2$.

Sample size	ParameterError				DecisionError				Regret			
	FY	SPA	KKA	VIA	FY	SPA	KKA	VIA	FY	SPA	KKA	VIA
50	1.26	1.24	4.19	2.08	2.18	2.23	9.16	3.96	0.11	0.12	1.07	0.29
100	0.82	0.86	4.61	1.88	1.48	1.65	9.62	3.66	0.05	0.06	1.16	0.23
300	0.47	0.73	4.87	1.79	0.87	1.46	9.86	3.58	0.02	0.04	1.22	0.18
500	0.35	0.70	4.92	1.78	0.67	1.43	9.92	3.57	0.01	0.03	1.23	0.17
1000	0.26	0.69	4.96	1.77	0.50	1.39	9.95	3.54	0.01	0.03	1.24	0.16

Table EC.8 The experimental results for various methods under different metrics are presented for the FOP defined as $\min\{(\theta + u)^\top x \mid x \in [-1, 1]^p\} = \min\{\sum_{k=1}^p (\theta_k + u_k)x_k \mid x \in [-1, 1]^p\}$ in the **Noisy Objective Function** setting. For the FY loss, we set $\lambda = 0.1$ and $\Omega(x) = 1/2\|x\|_2^2$.

Sample size	Parameter Error					Decision Error					Regret				
	FY	SPA	KKA	VIA	MOM	FY	SPA	KKA	VIA	MOM	FY	SPA	KKA	VIA	MOM
50	1.83	2.10	3.85	2.09	2.57	3.70	4.57	7.66	4.21	5.18	0.25	0.35	0.78	0.30	0.38
100	1.67	1.94	4.38	1.99	2.47	3.34	4.08	8.79	3.96	4.97	0.19	0.26	0.98	0.25	0.33
300	1.68	2.06	4.80	2.00	2.46	3.39	4.21	9.57	4.02	4.96	0.16	0.24	1.15	0.22	0.31
500	1.67	2.06	4.88	1.98	2.46	3.36	4.18	9.75	3.98	4.94	0.15	0.23	1.19	0.21	0.31
1000	1.69	2.08	4.93	2.01	2.46	3.39	4.20	9.86	4.04	4.93	0.15	0.23	1.22	0.21	0.31

Table EC.9 The experimental results for various methods under different metrics are presented for the FOP defined as $\min\{(\theta + u)^\top x \mid x \in [-1, 1]^p\} = \min\{\sum_{k=1}^p (\theta_k + u_k)x_k \mid x \in [-1, 1]^p\}$ in the **Noiseless** setting. For the FY loss, we set $\lambda = 0.01$ and $\Omega(x) = 1/2\|x\|_2^2$.

Sample size	Parameter Error					Decision Error					Regret				
	FY	SPA	KKA	VIA	MOM	FY	SPA	KKA	VIA	MOM	FY	SPA	KKA	VIA	MOM
50	0.31	0.55	0.39	0.34	1.78	0.00	1.04	0.80	0.46	3.34	0.00	0.03	0.02	0.07	0.16
100	0.15	0.62	0.20	0.19	1.74	0.01	1.26	0.40	0.14	3.36	0.00	0.03	0.00	0.04	0.15
300	0.06	0.71	0.06	0.07	1.69	0.03	1.45	0.13	0.04	3.37	0.00	0.03	0.00	0.00	0.14
500	0.04	0.70	0.04	0.04	1.70	0.03	1.42	0.08	0.02	3.38	0.00	0.03	0.00	0.00	0.14
1000	0.03	0.70	0.02	0.02	1.69	0.03	1.40	0.04	0.00	3.38	0.00	0.03	0.00	0.00	0.14

EC.4.1.4. Example D Then, we consider a nonlinear programming setting. The forward optimization problem(FOP) is

$$\min\{x^\top x - (\theta + u)^\top x \mid x \in [0, 1]^p\} = \max \left\{ -\sum_{k=1}^p x_k^2 + \sum_{k=1}^p (\theta + u)_k x_k \mid x_k \in [0, 1], \forall k \in [p] \right\}.$$

where context vector u follows a uniform distribution with support $[0, 2]^p$ and $p = 10$. We set the true parameter vector $\theta = [0.5, \dots, 0.5] \in \mathbb{R}^p$. The optimal solution to this problem can be expressed as

$$x^*(\theta; u)_k = \max \left(0, \min \left(1, \frac{(\theta + u)_k}{2} \right) \right).$$

To compute the Fenchel-Young loss, we first derive the convex conjugate of Ω , which is

$$\max_{x \in \mathcal{X}(u)} V_\lambda(\theta; u, x) = \max_{x \in [0, 1]^p} \sum_{k=1}^p \left\{ -x_k^2 + (\theta_k + u_k)x_k - \frac{\lambda}{2} x_k^2 \right\} \rightarrow x_\lambda^*(\theta; u)_k = \max \left\{ 0, \min \left\{ 1, \frac{\theta_k + u_k}{\lambda + 2} \right\} \right\}$$

Therefore, based on the observation solution y , we have the following expression of Fenchel-Young loss,

$$\begin{aligned} L_\lambda(\theta; u, y) &= \max_{x \in \mathcal{X}(u)} V_\lambda(\theta; u, x) + \lambda \Omega(y) - \left[-\sum_{k=1}^p (\theta_k + u_k) y_k \right] \\ &= \max_{x \in \mathcal{X}(u)} V_\lambda(\theta; u, x) + \lambda \Omega(y) + \sum_{k=1}^p (\theta_k + u_k) y_k \end{aligned}$$

Then, we have the gradient of Fenchel-Young Loss:

$$\nabla_{\theta_k} L_\lambda(\theta; u, y) = [x_\lambda^*(\theta; u)_k - y_k] = \left[\max \left\{ 0, \min \left\{ 1, \frac{\theta_k + u_k}{\lambda + 2} \right\} \right\} - y_k \right].$$

for $k = 1, \dots, p$.

Result Discussion The results of experiments in the Noisy Decision setting, the Noisy Objective Function setting, and the Noiseless setting, which are shown in Table EC.10, Table EC.11 and Table EC.12 respectively, average over 100 repetitions. Based on the above results, we can draw some interesting conclusions.

- In the Noisy Decision and Noisy Objective Function settings, the KKA method even fails to solve when using the Gurobi solver. However, in the Noiseless setting, KKA performs very well. In contrast, our Fenchel-Young loss method consistently outperforms other inverse optimization methods in all settings. This highlights the significant advantages of our method in solving inverse optimization problems, particularly when the forward optimization problem is nonlinear.

- In the Noiseless setting, both KKA and our method achieve zero decision error and regret. KKA exhibits the best overall performance, while our method closely follows with a low parameter error. In contrast, VIA performs the worst and does not converge. This may be attributed to the fact that the objective function in this problem is nonlinear with respect to the decision variable x . Since VIA employs a first-order conditional approximation, it can only guarantee the equivalence to ASO when the objective function is linear in x .

Table EC.10 The experimental results for various methods under different metrics are presented for the FOP defined as $\min\{x^\top x - (\theta + u)^\top x \mid x \in [0, 1]^p\} = \min\{\sum_{k=1}^p x_k^2 - \sum_{k=1}^p (\theta + u)_k x_k \mid x_k \in [0, 1], \forall k \in [p]\}$ in the **Noisy Decision** setting. For the FY loss, we set $\lambda = 0.1$ and $\Omega(x) = 1/2\|x\|_2^2$.

Sample size	Parameter Error				Decision Error				Regret			
	FY	SPA	KKA	VIA	FY	SPA	KKA	VIA	FY	SPA	KKA	VIA
50	2.33	2.90	-	7.94	0.14	0.21	-	0.74	0.15	0.22	-	0.74
100	1.57	2.05	-	8.01	0.07	0.12	-	0.75	0.07	0.12	-	0.75
300	0.92	1.52	-	7.79	0.02	0.07	-	0.74	0.02	0.07	-	0.74
500	0.70	1.44	-	7.64	0.01	0.06	-	0.72	0.01	0.06	-	0.72
1000	0.52	1.36	-	7.74	0.01	0.05	-	0.74	0.01	0.05	-	0.74

Table EC.11 The experimental results for various methods under different metrics are presented for the FOP defined as $\min\{x^\top x - (\theta + u)^\top x \mid x \in [0, 1]^p\} = \min\{\sum_{k=1}^p x_k^2 - \sum_{k=1}^p (\theta + u)_k x_k \mid x_k \in [0, 1], \forall k \in [p]\}$ in the **Noisy Objective Function** setting. For the FY loss, we set $\lambda = 0.1$ and $\Omega(x) = 1/2\|x\|_2^2$.

Sample size	Parameter Error				Decision Error				Regret			
	FY	SPA	KKA	VIA	FY	SPA	KKA	VIA	FY	SPA	KKA	VIA
50	1.37	2.52	-	8.80	0.05	0.15	-	0.85	0.05	0.16	-	0.85
100	1.26	2.67	-	8.29	0.04	0.15	-	0.80	0.04	0.16	-	0.80
300	1.28	2.88	-	5.85	0.03	0.17	-	0.51	0.04	0.18	-	0.51
500	1.28	2.89	-	4.57	0.03	0.17	-	0.37	0.03	0.18	-	0.37
1000	1.28	2.89	-	3.38	0.03	0.17	-	0.23	0.03	0.18	-	0.23

Table EC.12 The experimental results for various methods under different metrics are presented for the FOP defined as $\min\{x^\top x - (\theta + u)^\top x \mid x \in [0, 1]^p\} = \min\{\sum_{k=1}^p x_k^2 - \sum_{k=1}^p (\theta + u)_k x_k \mid x_k \in [0, 1], \forall k \in [p]\}$ under the **Noiseless** setting. For the FY loss, we set $\lambda = 0.1$ and $\Omega(x) = 1/2\|x\|_2^2$.

Sample size	Parameter Error				Decision Error				Regret			
	FY	SPA	KKA	VIA	FY	SPA	KKA	VIA	FY	SPA	KKA	VIA
50	0.07	1.26	0.00	13.29	0.00	0.03	0.00	1.33	0.00	0.03	0.00	1.33
100	0.06	1.31	0.00	13.53	0.00	0.03	0.00	1.35	0.00	0.04	0.00	1.35
300	0.06	1.32	0.00	14.66	0.00	0.03	0.00	1.40	0.00	0.04	0.00	1.40
500	0.06	1.32	0.00	14.82	0.00	0.03	0.00	1.41	0.00	0.04	0.00	1.41
1000	0.06	1.33	0.00	14.88	0.00	0.03	0.00	1.41	0.00	0.04	0.00	1.41

EC.4.1.5. Example E Finally, we consider the following forward optimization problem(FOP) with nonlinear constraint,

$$\min\{-(\theta + u)^\top x \mid \|x\|_2^2 \leq a^2\} = \min\left\{-\sum_{k=1}^p (\theta_k + u_k)x_k \mid \|x\|_2^2 \leq a^2\right\}.$$

where context vector u follows a uniform distribution with support $[0, 2]^p$ and $p = 10$. We set the true parameter vector $\theta = [0.5, \dots, 0.5] \in \mathbb{R}^p$ and $a = 3$. The optimal solution to this problem can be expressed as

$$x^*(\theta; u) = \frac{a(\theta + u)}{\|\theta + u\|_2}$$

To compute the Fenchel-Young loss, we first derive the convex conjugate of Ω , which is

$$\max_{x \in \mathcal{X}(u)} V_\lambda(\theta; u, x) = \max_{x \in \mathcal{F}} \left\{ (\theta + u)^\top x - \frac{\lambda}{2} x^\top x \right\} \rightarrow x_\lambda^*(\theta; u) = \begin{cases} \frac{\theta + u}{\lambda}, & \text{if } \lambda \geq \frac{\|\theta + u\|_2}{a} \\ \frac{a(\theta + u)}{\|\theta + u\|_2}, & \text{if } \lambda < \frac{\|\theta + u\|_2}{a}. \end{cases}$$

where feasible set $\mathcal{F} : \{x \in \mathbb{R}^p \mid \sum_{i=1}^p x_i^2 \leq a^2\}$. Based on the observation solution y , we have the following expression of Fenchel-Young loss,

$$\begin{aligned} L_\lambda(\theta; u, y) &= \max_{x \in \mathcal{X}(u)} V_\lambda(\theta; u, x) + \lambda\Omega(y) - \left[\sum_{k=1}^p (\theta_k + u_k)y_k \right] \\ &= \max_{x \in \mathcal{X}(u)} V_\lambda(\theta; u, x) + \lambda\Omega(y) - \sum_{k=1}^p (\theta_k + u_k)y_k \end{aligned}$$

Thus, we have the gradient of Fenchel-Young Loss:

$$\nabla_{\theta_k} L_\lambda(\theta; u, y) = [x_\lambda^*(\theta; u)_k - y_k]$$

for $k = 1, \dots, p$.

Result Discussion The results of experiments in the Noisy Decision setting, the Noisy Objective Function setting, and the Noiseless setting, which are shown in Table EC.13, Table EC.14 and Table EC.15 respectively, average over 100 repetitions. Based on this information, we can draw the following conclusions.

- In the Noisy Decision and Noisy Objective Function settings, only our method based on the Fenchel-Young loss can be effectively solved using Gurobi, while other inverse optimization methods, except KKA, fail to provide effective solutions. Although KKA can be solved, the results do not converge. This highlights the robustness and efficiency of our Fenchel-Young loss method in handling inverse optimization problems with noisy data and nonlinear constraints, which are common challenges in this domain.

• In the Noiseless setting, the VIA method demonstrates the best performance, achieving a perfect estimation of the parameter vector θ when the sample size was equal to 50. Furthermore, both its decision error and regret are zero. However, as the sample size increases, the computational time exceeds practical limits, preventing the acquisition of results. Consequently, these cases were not recorded in the table.

In addition, KKA fails to converge under the Noiseless setting, resulting in substantial parameter error, decision error, and regret. However, our proposed method continues to deliver near-perfect results with rapid convergence. Specifically, the parameter error is remarkably low, while the decision error and regret are both zero.

Table EC.13 The experimental results for various methods under different metrics are presented for the FOP defined as $\min\{-(\theta + u)^\top x \mid \|x\|_2^2 \leq a^2\} = \min\{-\sum_{k=1}^p (\theta_k + u_k)x_k \mid \|x\|_2^2 \leq a^2\}$ in the **Noisy Decision** setting. For the FY loss, we set $\lambda = 0.1$ and $\Omega(x) = 1/2\|x\|_2^2$.

Sample size	Parameter Error				Decision Error				Regret			
	FY	SPA	KKA	VIA	FY	SPA	KKA	VIA	FY	SPA	KKA	VIA
50	1.02	-	4.59	-	0.24	-	1.08	-	0.09	-	0.38	-
100	0.67	-	4.80	-	0.11	-	1.13	-	0.04	-	0.40	-
300	0.39	-	4.93	-	0.04	-	1.16	-	0.01	-	0.41	-
500	0.30	-	4.96	-	0.02	-	1.17	-	0.01	-	0.42	-
1000	0.23	-	4.98	-	0.01	-	1.18	-	0.00	-	0.42	-

Table EC.14 The experimental results for various methods under different metrics are presented for the FOP defined as $\min\{-(\theta + u)^\top x \mid \|x\|_2^2 \leq a^2\} = \min\{-\sum_{k=1}^p (\theta_k + u_k)x_k \mid \|x\|_2^2 \leq a^2\}$ in the **Noisy Objective Function** setting. For the FY loss, we set $\lambda = 0.1$ and $\Omega(x) = 1/2\|x\|_2^2$.

Sample size	Parameter Error				Decision Error				Regret			
	FY	SPA	KKA	VIA	FY	SPA	KKA	VIA	FY	SPA	KKA	VIA
50	0.51	-	4.59	-	0.04	-	1.08	-	0.01	-	0.38	-
100	0.50	-	4.80	-	0.03	-	1.13	-	0.01	-	0.40	-
300	0.49	-	4.93	-	0.03	-	1.16	-	0.01	-	0.41	-
500	0.50	-	4.96	-	0.03	-	1.17	-	0.01	-	0.42	-
1000	0.50	-	4.98	-	0.03	-	1.18	-	0.01	-	0.42	-

Table EC.15 The experimental results for various methods under different metrics are presented for the FOP defined as $\min\{-(\theta + u)^\top x \mid \|x\|_2^2 \leq a^2\} = \min\{-\sum_{k=1}^p (\theta_k + u_k)x_k \mid \|x\|_2^2 \leq a^2\}$ in the **Noiseless** setting. For the FY loss, we set $\lambda = 0.1$ and $\Omega(x) = 1/2\|x\|_2^2$

Sample size	Parameter Error				Decision Error				Regret			
	FY	SPA	KKA	VIA	FY	SPA	KKA	VIA	FY	SPA	KKA	VIA
50	0.04	-	4.59	0.00	0.00	-	1.08	0.00	0.00	-	0.38	0.00
100	0.04	-	4.80	-	0.00	-	1.13	-	0.00	-	0.40	-
300	0.04	-	4.93	-	0.00	-	1.16	-	0.00	-	0.41	-
500	0.04	-	4.96	-	0.00	-	1.17	-	0.00	-	0.42	-
1000	0.03	-	4.98	-	0.00	-	1.18	-	0.00	-	0.42	-

EC.4.1.6. Computational Time In this section, we present a concise summary of the total computational time for 100 serial runs of the synthetic data experiments under various settings and sample sizes. Taking the Noisy Decision setting as an example, the results for other settings are similar, and the detailed findings are shown in Table EC.16. The units of the numbers in the table are seconds. From these results, the following conclusions can be readily drawn.

- **Computational Efficiency of Our Method:** Except for Example A, our method consistently achieves the shortest computational time across all experiments with an order-of-magnitude improvement, typically requiring only a few seconds to complete the entire computation in most experiments. In contrast, other methods generally take at least tens of seconds or more. Additionally, as the sample size increases, the growth rate of computational time for our method remains manageable. In Example A, the explicit gradient expression of the Fenchel-Young loss cannot be derived, necessitating the use of a solver, which slows down the computation. However, by tuning the parameters of stochastic gradient descent, we can still complete the computation within an acceptable time frame, even with a large sample size.

- **Computational Bottleneck of SPA:** In all experiments, SPA exhibits the longest computational time among all methods. This is attributed to its use of a semi-parametric algorithm for noise removal. According to relevant literature Aswani et al. (2018), the semi-parametric algorithm requires cross-validation for hyperparameter tuning, which significantly increases the computational time compared to KKA and VIA.

- **Comparable Computational Time of KKA and VIA:** The computational time for KKA and VIA remains on the same order of magnitude across all experiments. Except for Example A, their computational times are significantly higher than that of our method but considerably lower than that of SPA.

Table EC.16 computational time results of different methods in each experiments under **Noisy Decision** setting.

Sample size		50	100	300	500	1000
Example A	FY	20.34	21.54	68.33	64.13	97.20
	SPA	290.84	409.33	710.18	1858.89	3574.48
	KKA	2.92	9.76	13.76	26.71	49.82
	VIA	2.19	15.09	26.11	41.70	78.80
Example B	FY	0.75	0.85	1.54	2.28	4.39
	SPA	62.54	122.73	504.12	1064.74	3906.52
	KKA	3.09	6.52	20.73	37.43	70.86
	VIA	2.41	3.42	32.94	37.02	36.83
Example C	FY	0.72	0.77	1.25	1.85	3.25
	SPA	166.96	140.48	507.64	1024.51	3205.72
	KKA	3.38	7.78	20.12	32.53	62.99
	VIA	1.98	8.02	15.05	24.34	54.06
Example D	FY	0.65	0.76	1.30	1.97	3.43
	SPA	86.24	159.85	590.19	1780.07	4481.71
	KKA	-	-	-	-	-
	VIA	13.62	9.93	38.16	76.80	204.85
Example E	FY	1.94	3.73	14.98	35.67	38.22
	SPA	-	-	-	-	-
	KKA	42.46	257.40	907.82	2486.15	21449.75
	VIA	-	-	-	-	-

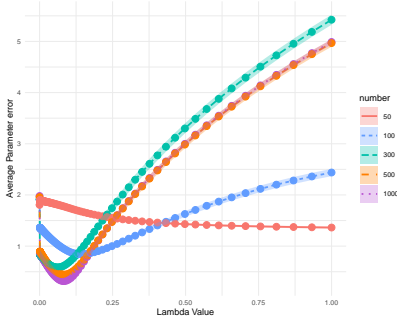


Figure EC.1 Example A PE

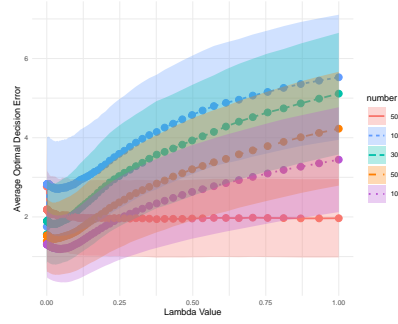


Figure EC.2 Example A DE

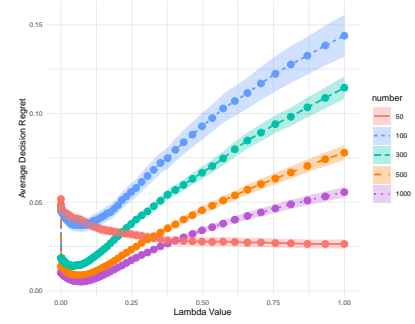


Figure EC.3 Example A regret

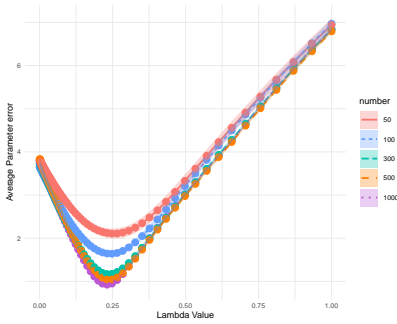


Figure EC.4 Example B PE

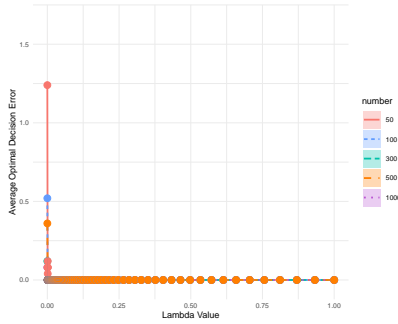


Figure EC.5 Example B DE

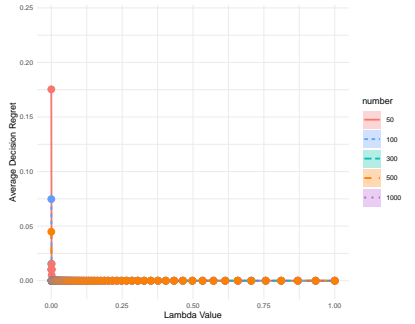


Figure EC.6 Example B regret

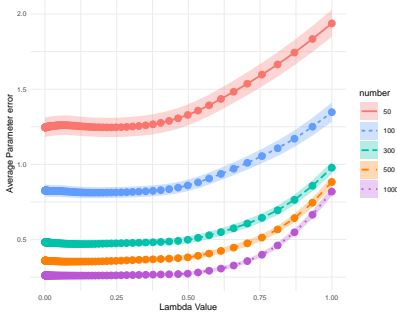


Figure EC.7 Example C PE

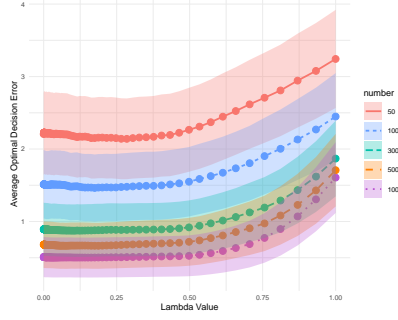


Figure EC.8 Example C DE

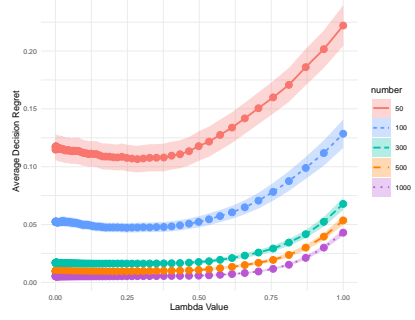


Figure EC.9 Example C regret

EC.4.1.7. Sensitivity Analysis In this section, we investigate the impact of the regularization parameter λ on various metrics when solving inverse optimization problems using our method. Specifically, for all experiments except Example E, we select regular coefficient λ from a grid of 0 and 100 points distributed uniformly on the logarithmic scale over 0.001 to 1. For Example E, we select regular coefficient λ from a grid of 0 and 100 points distributed uniformly on the logarithmic scale over 0.005 to 5.

From Figure EC.1 to Figure EC.15, we present the results of the Fenchel-Young loss for different λ values in each synthetic data experiment under the Noisy Decision setting, along with the corresponding 95% confidence intervals derived from 100 repeated experiments. In the titles of these

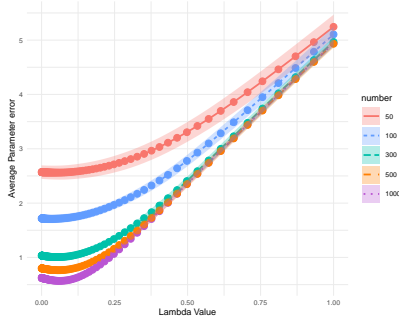


Figure EC.10 Example D PE

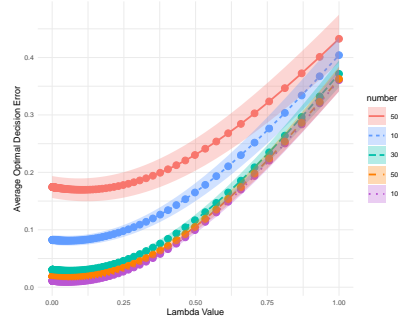


Figure EC.11 Example D DE

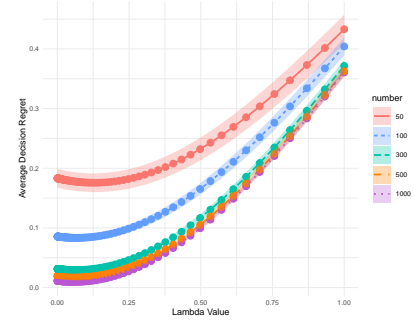


Figure EC.12 Example D regret

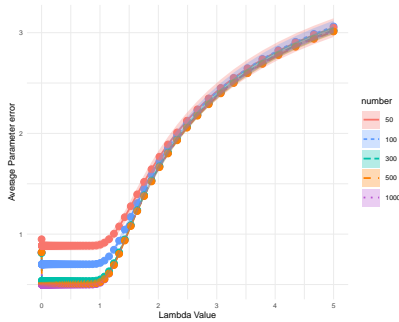


Figure EC.13 Example E PE

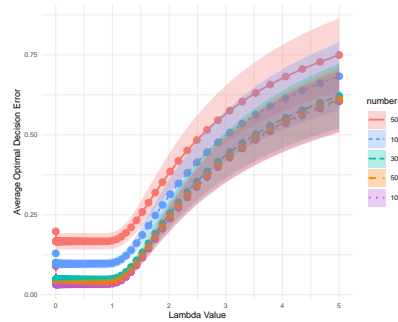


Figure EC.14 Example E DE

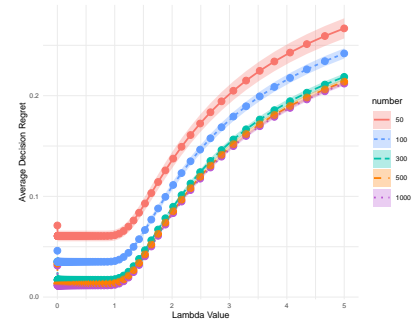


Figure EC.15 Example E regret

figures, **PE** denotes Parameter Error, while **DE** denotes Decision Error. Based on these results, we draw the following conclusions.

- For Example A, When the sample size is 50, the parameter error, decision error, and regret gradually decrease as λ increases. This indicates that when the sample size is insufficient, a sufficiently strong regularization is beneficial for better performance. When the sample size exceeds 50, these three metrics first decrease and then increase with the increase of λ , showing a V-shaped pattern. This suggests that when the sample size is adequate, excessive regularization introduces significant bias, which is detrimental to performance enhancement. For parameter error, the optimal λ value varies with different sample sizes. In contrast, for decision error and regret, the optimal λ value remains almost the same across different sample sizes.

In summary, this example primarily illustrates that the selection of the optimal λ value requires a comprehensive consideration of multiple factors, including sample size and specific metrics. Moreover, in all three figures, there is a sharp drop when λ transitions from 0 to a non-zero value, highlighting the necessity and rationality of regularization.

- For Example B, the parameter error curve exhibits a distinct V-shape. Specifically, as the value of λ increases, the parameter error initially decreases and then subsequently increases. The minimum point is approximately at $\lambda = 0.25$, and as the sample size increases, this minimum point shifts slightly to the left. This trend is reasonable because, with a larger sample size, the optimal value of the regularization term should gradually decrease.

Moreover, in this example, the decision error and regret curves clearly illustrate the benefits of regularization. When $\lambda = 0$, the solution obtained is far from optimal, and the regret is substantial. However, once $\lambda > 0$, the solution immediately becomes nearly optimal.

In summary, this example demonstrates that regularization is both helpful and necessary. Even a small value of λ can significantly outperform a value of 0. Additionally, proper selection of λ can facilitate parameter recovery.

- For Example C, it is observed that when the value of λ lies between 0 and 0.5, the three metrics under consideration remain relatively stable overall. Specifically, when the sample size is 50, the regret exhibits a slight trend of initially decreasing and then increasing, with the lowest point occurring around $\lambda = 0.3$.

However, when the value of λ exceeds 0.5, the three metrics show a significant upward trend. This is reasonable because an excessively large regularization coefficient λ introduces substantial bias, leading to poor performance. Additionally, as the sample size increases, the values of the three metrics decrease, which is expected.

In summary, this example demonstrates that our method allows for a broad range of λ values. As long as λ is not excessively large, it can ensure effective parameter recovery and satisfactory decision-making performance.

- For Example D, compared to Example C, its objective function includes a quadratic term $x^\top x$, and the term $(\theta + u)$ is modified to $-(\theta + u)$. Similar to Example C, when the λ value is very small, specifically around 0 to 0.1, the curves for parameter error, decision error, and regret are relatively smooth. However, when the value of λ exceeds 0.1, these metrics increase rapidly. Additionally, when the sample size is 50, the regret initially decreases slightly before increasing. This may be because, when the sample size is insufficient, appropriate regularization helps to reduce regret.

In summary, this example illustrates that when dealing with nonlinear programming, the choice of λ may need to be more carefully considered compared to linear programming, with values closer to 0 being more appropriate.

- For Example E, we specifically adjust the λ value selection range to 0.005 to 5 instead of 0.001 to 1, just to show the two phase transitions in this experiment. First, we find that there is a jump at the point where $\lambda = 0$. In other words, when $\lambda = 0$ becomes $\lambda > 0$, parameter error, decision error and regret will suddenly decrease, which reflects the advantages of regularization. For λ values are less than 1, the three metrics we consider remain at a very stable and very low level. Reviewing the previous discussion of this example, we can see that the reason for this is that when λ is less than $\frac{\|\theta+u\|_2}{a}$, $x^*(\theta, u) = \frac{a(\theta+u)}{\|\theta+u\|_2}$ is a fixed constant and our algorithm is not affected in any way. Only when λ is greater than $\frac{\|\theta+u\|_2}{a}$ does $x^*(\theta, u) = \frac{\theta+u}{\lambda}$ change with λ . Consequently, when λ is greater than 1,

the phase transition occurs again. Due to the introduction of large bias, parameter error, decision error and regret will rise rapidly with the increase of λ .

In general, this example demonstrates the unique properties of our method in the ball constraint space. When regularization is present and the value is below a certain threshold, our method ensures a very stable and relatively optimal performance.

EC.4.1.8. Synthetic Data Experiment Conclusions In summary, our method is gradient-based, whereas other classical inverse optimization methods are primarily model-based. This fundamental difference endows our approach with unique advantages in several key aspects:

- **Avoid Degeneracy:** When optimization parameters are estimated using model-based inverse optimization methods, degenerate solutions (e.g., an all-zero vector in Example B) may arise, leading to meaningless optimal solutions and ineffective decision-making. Our Fenchel-Young loss-based method circumvents this issue, ensuring robust decision performance.

- **Handling Noise More Effectively:** Many classical inverse optimization methods perform well only in noiseless settings. In noisy environments, solver failures are common. In contrast, our method remains stable regardless of noise, yielding accurate parameter estimates and satisfactory decision outcomes.

- **Effective Acceleration:** Our method exhibits significant computational advantages over other inverse optimization methods. Although we cannot derive an explicit expression for the optimal solution $x_\lambda^*(\theta; u)$ of the conjugate function $\max_{x \in \mathcal{X}(u)} V_\lambda(\theta; u, x)$ in Example A, we can employ stochastic gradient descent to maintain acceptable computational time, even with large sample sizes. Conversely, the computational time for other classical methods increases sharply with increasing sample size. These methods, being model-based, incorporate each data point as a constraint, thereby exponentially increasing the complexity of optimization problem. Moreover, there is no systematic approach to accelerate these calculations.

EC.4.2. Real Data Experiment Setup and Implementation details

In this section we study our Fenchel-Young loss method and baselines empirically to demonstrate the great advantages of our method in solving inverse optimization problems in practical applications. The real data we use are collected from Uber Movement(<https://movement.uber.com>), which describes the traveling times data in Los Angeles. In our experiment, We mainly focus on 45 census tracts in downtown Los Angeles, collecting historical data of average traveling times from each of these census tracts to its neighbors, which includes 93 edges, during five periods in each day (AM Peak, Midday, PM Peak, Evening, Early Morning) in 2018 and 2019. Next, we will introduce our experiment from the following aspects.

- **Forward optimization problem(FOP) and observed solution:** Our objective is to determine an optimal path from the easternmost census tract(Aliso Village) to the westernmost census tract(MacArthur Park), which is encoded by $x \in \{0, 1\}^d$ with $d = 93$. More detailed setting can be found in Kallus and Mao (2023). When $x_j = 1$, it means that we travel on edge j . Because our forward optimization problem is actually the shortest path problem on a graph with 45 nodes and 93 edges. Therefore, we also need to consider the flow preservation constraints, which are denoted as $Ax = b, A \in \mathbb{R}^{45 \times 93}, b \in \mathbb{R}^{45}$.

Furthermore, to construct an inverse optimization problem, we solve for a shortest path based on the travel time of each edge at each data point in the dataset, which serves as the observed optimal solution Y . The travel times vector for 93 edges is modeled as θu , where $\theta \in \mathbb{R}^{93 \times 12}$ and $u \in \mathbb{R}^{12}$. 12 means that the dimension of the context vector of each piece of data is 12, which we will describe in detail in the next paragraph. Finally, the forward optimization problem(FOP) is shown below.

$$\min_x \left\{ \sum_{k=1}^{93} (\theta_k u) x_k \mid Ax = b \right\}.$$

θ_k is the k-th row of the matrix θ . The objective of inverse optimization is to find a parameter matrix $\theta \in \mathbb{R}^{93 \times 12}$ and estimate c by θu , so as to obtain a good decision on the test set data that is close enough to the observed optimal solution or low enough to the regret.

- **Context vector:** We totally consider 7 covariates including wind speed, visibility and other calendar features, which can be regarded as context vector u for over inverse optimization problem. To be more precise, we process the period feature with one-hot encoder and add the intercept term, and the final processed context vector is $u \in \mathbb{R}^{12}$.

- **Other experimental details:** We divide the datasets into four distinct time spans: half a year (920 data points), one year (1825 data points), one and a half years (2735 data points), and two years (3640 data points). For each dataset, we randomly select 40% of the data as the test set and 60% as

the training set. Each set of experiments is run in parallel across 30 replications, and we collect the average computational time, the average relative regret ratio, and the average decision error.

The relative regret ratio means that the regret on the test set is divided by the traveling time of the optimal decision, which can represent the percentage of time that the outcome of the decision takes longer than the optimal decision. The definition of decision error is exactly the same as in the previous synthetic data experiments.

Next, we delve into the specifics of how our method addresses these inverse optimization problems. To compute the Fenchel-Young loss, we first derive the convex conjugate of Ω , which is

$$\max_{x \in \mathcal{X}(u)} V_\lambda(\boldsymbol{\theta}; u, x) = \max_{x \in \mathcal{F}} \left\{ \sum_{k=1}^{93} (\boldsymbol{\theta}_k u) x_k - \frac{\lambda}{2} x^\top x \right\} \rightarrow x_\lambda^*(\boldsymbol{\theta}; u).$$

where feasible set $\mathcal{F} : \{x \in \{0, 1\}^{93} | Ax = b\}$. As in Example A, we still cannot directly write an explicit expression for x in this problem, so we need to utilize the solver to solve it. In order to ensure the efficiency of the gradient calculation, we still adopt the stochastic gradient descent algorithm, but different from Example A, we need to calculate that the gradient of $\boldsymbol{\theta}$ is a matrix rather than a vector, so we need to pay attention to the dimension matching. The details of gradient calculation are shown below.

Based on the observation solution y , we have the following expression of Fenchel-Young loss,

$$\begin{aligned} L_\lambda(\boldsymbol{\theta}; u, y) &= \max_{x \in \mathcal{X}(u)} V_\lambda(\boldsymbol{\theta}; u, x) + \lambda \Omega(y) - \left[- \sum_{k=1}^{93} (\boldsymbol{\theta}_k u) y_k \right] \\ &= \max_{x \in \mathcal{X}(u)} V_\lambda(\boldsymbol{\theta}; u, x) + \lambda \Omega(y) + \sum_{k=1}^{93} (\boldsymbol{\theta}_k u) y_k \end{aligned}$$

Thus, we have the gradient of Fenchel-Young Loss:

$$\nabla_{\boldsymbol{\theta}} L_\lambda(\boldsymbol{\theta}; u, y) = [-x_\lambda^*(\boldsymbol{\theta}; u) + y] u^\top$$

Result Discussion The results of this real data experiment are shown in Table EC.17. Occasionally, the VIA method fails to solve the problem. In such cases, we set $\boldsymbol{\theta}$ to be a matrix of all zeros, resulting in a random selection of a feasible path as the decision. Given that the forward optimization problem (FOP) for this problem is a linear programming problem and the observed solutions are noise-free, the maximum optimality margin (MOM) method is applicable. Based on the experimental results, we draw the following conclusions.

- For decision error, our method achieves the lowest decision error, significantly outperforming other methods. This indicates that, regardless of the time span, the optimal path identified by our method closely approximates the true optimal path. The second-best performance is observed with the MOM method, which consistently ensures that the selected path is near-optimal. In contrast, the SPA, VIA, and KKA methods exhibit suboptimal performance, with substantial deviations from the true optimal solution.

Table EC.17 Real data experiment results. Numbers in the **Relative Regret Ratio** column mean percentages.

For example, 1.01 means a relative regret ratio of 1.01%. The number in the **Period** column means years. For example, 1.5 means that the data set used spans one and a half years. The number in the **Computational time** column means seconds. For example, 6 means that the average running time of the method is 6 seconds. For

Fenchel-Young loss, we set $\lambda = 0.1$ and $\Omega(x) = 1/2\|x\|_2^2$.

Period (years)	Decision Error					Relative Regret Ratio (%)					Computing time (seconds)				
	FY	SPA	KKA	VIA	MOM	FY	SPA	KKA	VIA	MOM	FY	SP	KKA	VIA	MOM
0.5	2.06	6.80	5.41	10.72	3.58	1.01	29.51	8.30	34.51	4.87	6	120	66	59	438
1	2.00	6.72	6.61	11.77	4.09	0.97	29.55	12.39	41.51	4.96	8	287	152	107	647
1.5	1.97	6.77	7.09	7.33	4.66	0.94	29.50	12.81	30.95	4.21	9	513	242	185	901
2	1.89	6.78	7.07	7.17	4.64	0.84	29.28	12.40	30.41	3.26	11	839	281	256	1218

- For relative regret ratio, our method exhibits significant advantages over other methods again. This indicates that the path travel time provided by our method is very close to the optimal path travel time. The second-best performance is observed with the MOM method, which also performs well and maintains a relatively low regret ratio. Although KKA has a high decision error, its relative regret ratio is marginally satisfactory. In contrast, the performance of SPA and VIA remains poor, with high relative regret ratios.

- For computational time, our method exhibits the shortest computational time compared to other methods, which are significantly longer. Other methods involve solving complex optimization problems with constraints that grow with the amount of data. Given the large volume of real data, these methods require extensive computational resources and time to reach a solution. In contrast, our method only requires a finite number of gradient descent steps, and computing the gradient involves solving relatively simple optimization problems. As a result, our method offers a substantial advantage in terms of computational speed.